

AD-A083 908

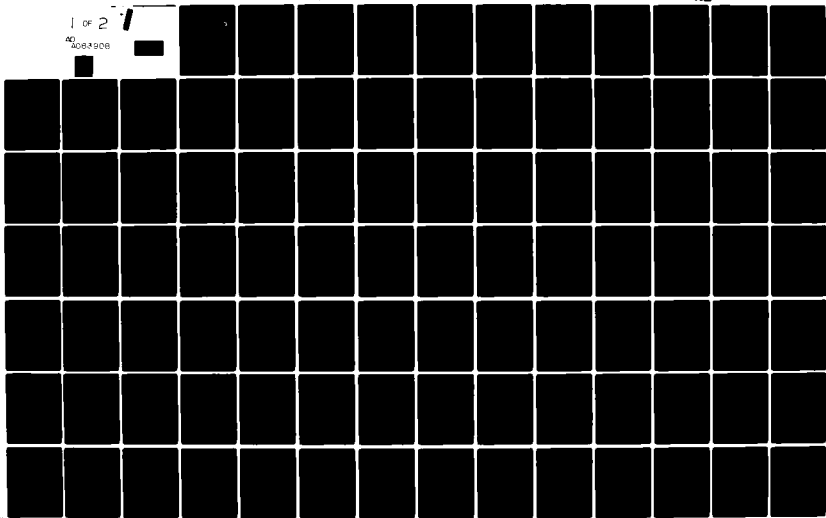
AIR FORCE INST OF TECH WRIGHT-PATTERSON AFB OH SCHOO
ADDITION OF AN AEROSOL TRANSMISSION MODEL TO THE AERONAUTICAL
MAR 79 A C MCLELLAN
AFIT/6AE/AA/79M-3

NL

UNCLASSIFIED

1 of 2

AD
A083908



AFIT/GAE/AA/79M-3

1

DTIC
MAY 8 1980
C

6

ADDITION OF AN AEROSOL TRANSMISSION MODEL
TO THE AERONAUTICAL SYSTEMS DIVISION
INFRA-RED EMISSION PREDICTION PROGRAM
(ASDIR).

9

Master

THESIS,

14

AFIT/GAE/AA/79M-3

10

Allen C. McLellan
Capt USAF

11, Mar 79

12 112

Approved for public release; distribution unlimited.

AFIT/GAE/AA/79M-3

ADDITION OF AN AEROSOL TRANSMISSION MODEL
TO THE AERONAUTICAL SYSTEMS DIVISION
INFRA-RED EMISSION PREDICTION PROGRAM
(ASDIR)

THESIS

Presented to the Faculty of the School of Engineering
of the Air Force Institute of Technology
Air Training Command
in Partial Fulfillment of the
Requirements for the Degree of
Master of Science

by

Allen C. McLellan, B.S.A.E.

Captain USAF

Graduate Aerospace Engineering

March 1979

Approved for public release; distribution unlimited.

Acknowledgments

The subject of this study was suggested by Mr. Stan Tate of the Aeronautical Systems Division of Wright-Patterson AFB, OH. As one of the authors of ASDIR he has been of invaluable assistance throughout the course of the project. Even though his is an exceptionally heavy workload he has maintained an admirable zest and enthusiasm for this work and offered advice and encouragement at every turn. Certainly without his help this project would not have been completed; I express my sincere appreciation to Mr. Tate.

Dr. James E. Hitchcock served as my thesis advisor at the Air Force Institute of Technology and provided valuable insight and direction at several stages in this effort and pertinent, constructive criticisms in preparation of the final report. I also wish to thank personnel of the Systems Research Laboratories of Dayton, especially Mr. Paul Zidek and Mr. Ira Bowker, who were very gracious in providing results of their work in programming LOWTRAN for a desk-top computer. Their excellent results provided a much-needed stimulus for my work in its early stages. A debt of gratitude is also owed to Major Pete Soliz of the Air Force Avionics Lab Weather Division for his help in obtaining well-formatted plots of LOWTRAN and ASDIR results. Dr. R. E. Roberts of the Institute for Defense Analysis is also to be thanked for taking time out for a telephone

discussion and sending his own unpublished material to aid in my project. Mrs. Molly Bustard of the AFIT Library staff provided exceptional service in locating research material for the study.

The biggest share of appreciation must go to my loving wife, Faye, who has patiently given unselfish support and understanding throughout nearly six years of marriage. Especially in the last 18 months she has stood beside me, encouraged me, and been truly one with me. Additionally, she has given me Tara, a joyous little girl, who adds a whole new dimension to our lives. God in heaven has blessed us abundantly - certainly "all things work together for good to them that love God, to them who are called according to His purpose" (Romans 8:28).

Accession For	
WHS GR&I	<input checked="" type="checkbox"/>
Mr. TAB	<input type="checkbox"/>
Unannounced	
Justification	
By	
Distribution/	
Available to	
Dist. to	Special
A	

Contents

	Page
Acknowledgments	ii
List of Figures	vi
List of Tables	viii
Abstract	ix
I Introduction	1
II Background and Theory	7
ASDIR - IR Emission Prediction Program	7
Hot Surface Emission	9
External Surface Emissions	12
Plume Emissions and Atmospheric Attenuation	13
Atmospheric Aerosols	17
Sources of Atmospheric Aerosols	18
Dust-Like (Non-Hygroscopic) Particles	19
Hygroscopic Particles	20
Particle Removal Processes	21
Particle Composition	23
Particle Sizes	24
Measured Particle Size Distributions	29
Aerosol Vertical Distributions	33
Complex Index of Refraction	37
Extinction of IR Energy in the Atmosphere	40
Aerosol Extinction	43
LOWTRAN - AFGL Transmission Model	46
LOWTRAN - A General Description	47
LOWTRAN Calculation of Individual Transmittances	49
LOWTRAN Aerosol Treatment	49
LOWTRAN Aerosol Interpolation/ Extrapolation Scheme	51
III Results and Discussion	57
Particle Densities	57
Extinction Coefficients	60
Equivalent Sea Level Path Lengths	60
Aerosol Transmission Calculations	63
Comparison of the Unmodified ASDIR and LOWTRAN	72
Addition of the HAZE Subroutine into ASDIR	72
Concluding Remarks	76

	Page
Bibliography	82
Appendix A: A Short Summary of Mie Theory and Calculations	84
Appendix B: Derivation of Expressions for Equivalent Path Lengths	92
Appendix C: Program Listings of Subroutine HAZE, AVCAL, and BETCAL	96
Vita	99

List of Figures

Figure	Page
1 Aircraft IR Radiation Sources	8
2 Relative Importance of Contributions to a Weapon Systems Infrared Signature	10
3 SIGNIR Flowchart as Used in ASDIR	11
4 ASDIR Ray Geometry	14
5 Size Ranges of Aerosols	25
6 Size Distribution of Aerosol Particles with Coagulation Affecting the Lower Size Range	27
7 Average Size Distribution for Continental Aerosols Near the Earth's Surface	32
8 Geometry of Slant Paths in the Plane- Parallel Approximation for Calculating Equivalent Path Lengths	36
9 Vertical Profiles of Particle Concentration from Elterman (1964, 1968)	38
10 LOWTRAN Prediction Chart for Water Vapor Transmittance (4-26 μm)	50
11 LOWTRAN Average Continental Aerosol Extinc- tion Coefficients (Sea Level Values)	53
12 LOWTRAN Maritime Aerosol Extinction Coefficients (Sea Level Values)	54
13 Assumed Aerosol Vertical Distributions	58
14 LOWTRAN/HAZE Subroutine Comparison (2-6 μm)	64
15 LOWTRAN/HAZE Subroutine Comparison (2-6 μm)	64
16 LOWTRAN/HAZE Subroutine Comparison (2-6 μm)	65
17 LOWTRAN/HAZE Subroutine Comparison (2-6 μm)	65
18 LOWTRAN/HAZE Subroutine Comparison (2-6 μm)	66
19 LOWTRAN/HAZE Subroutine Comparison (2-6 μm)	66

Figure	Page
20 LOWTRAN/HAZE Subroutine Comparison (2-6 μm) . . .	67
21 LOWTRAN/HAZE Subroutine Comparison (2-6 μm) . . .	67
22 LOWTRAN/HAZE Subroutine Comparison (8-12 μm) . . .	68
23 LOWTRAN/HAZE Subroutine Comparison (8-12 μm) . . .	68
24 LOWTRAN/HAZE Subroutine Comparison (8-12 μm) . . .	69
25 LOWTRAN/HAZE Subroutine Comparison (8-12 μm) . . .	69
26 LOWTRAN/HAZE Subroutine Comparison (8-12 μm) . . .	70
27 LOWTRAN/HAZE Subroutine Comparison (8-12 μm) . . .	70
28 LOWTRAN/HAZE Subroutine Comparison (8-12 μm) . . .	71
29 LOWTRAN/HAZE Subroutine Comparison (8-12 μm) . . .	71
30 Low Altitude Comparison (Case 1) Between the Unmodified ASDIR and LOWTRAN Program Results . . .	73
31 Low Altitude Comparison (Case 2) Between the Unmodified ASDIR and LOWTRAN Program Results . . .	74
32 High Altitude Comparison (Case 3) Between the Unmodified ASDIR and LOWTRAN Program Results . . .	75
33 Modified ASDIR and LOWTRAN Comparison - Aerosol Transmission (2-6 μm)	77
34 Modified ASDIR and LOWTRAN Comparison - Total Transmission (2-6 μm)	78
35 Modified ASDIR and LOWTRAN Comparison - Aerosol Transmission (2-6 μm)	79
36 Modified ASDIR and LOWTRAN Comparison - Total Transmission (2-6 μm)	80
37 LOWTRAN Values of Equivalent Sea Level Path Lengths for Vertical Paths (AV(z))	93

List of Tables

Table	Page
I Aerosol Models. Vertical Distributions for a "Clear" and "Hazy" Atmosphere	52
II Derived Expressions for Particle Density	59
III Curve Fit Expressions for LOWTRAN Average Continental Aerosol Extinction Coefficients	61
IV Curve Fit Expressions for LOWTRAN Maritime Aerosol Extinction Coefficients	61

Abstract

The Aeronautical Systems Division Infra-Red Emission Prediction Program (ASDIR) is a large computer program compiled in 1974-75 using "state of the art" routines to predict hot surface and plume emission from a geometrically modeled target. The atmospheric transmission segment of the program included only the major gaseous absorbers (H_2O , CO_2 , and N_2) with no aerosol attenuation. To improve the flexibility of the program in making more accurate predictions at low altitudes, an aerosol transmission computational scheme was written for the ASDIR code.

Using the basic methodology in the Air Force Geophysics Laboratory (AFGL) transmission model LOWTRAN 4, a subroutine was written for direct inclusion into ASDIR. Curve fits of the following LOWTRAN parameters were performed which simplified the aerosol procedures and minimized the additional computer storage and time requirements in ASDIR: (1) assumed aerosol particle densities, (2) equivalent sea level path lengths for vertical paths - $AV(z)$, (3) total sea level extinction coefficients for an "average continental" and "maritime" aerosol models. Results of the new subroutine (called HAZE) compared very well with LOWTRAN's aerosol predictions. A logic change was included in HAZE to automatically select a maritime aerosol model under low visibility conditions. This programming change was prompted by results of a recent Grafenwohr, FRG transmission study.

ADDITION OF AN AEROSOL TRANSMISSION MODEL
TO THE AERONAUTICAL SYSTEMS DIVISION
INFRA-RED EMISSION PREDICTION PROGRAM
(ASDIR)

I. Introduction

In recent years, applications of infrared technology have multiplied in the Air Force and other services. Of special significance have been methods to determine the IR "signatures" of military targets, especially aircraft. The Aeronautical Systems Division Infra-Red Emission Prediction Program (ASDIR) is a large computer model used by ASD and civilian contractors in a wide range of IR engineering applications. Using a geometric representation of the subject aircraft, along with engine physical characteristics and operating parameters, the program computes emissions from hot exhaust surfaces and the exhaust plume. ASDIR then estimates the propagation of that energy through an attenuating atmosphere to an observer (usually an IR detector). With specific detector characteristics, a prediction can be made as to whether the target could be detected at a given range, altitude and viewing angle.

A serious complicating factor in such predictive schemes is atmospheric attenuation of the IR energy.

The energy is absorbed and scattered by both the molecules of the air and by atmospheric aerosols such as dust, smoke, and salt particles. The total effect of the atmospheric constituents can be approximated by the effects of the separate attenuators. The attenuating mechanisms of molecular scattering, molecular absorption (especially by H₂O and CO₂), and aerosol scattering and absorption can be related to meteorological parameters such as temperature, pressure, relative humidity, and particle density. Then, in theory, one can predict the cumulative attenuation of radiation as a function of the path and meteorological observables.

Aerosol attenuation is the least understood of the attenuating mechanisms listed above. The aerosol environment in any location is a result of complex aerosol production and removal processes, relative humidity, and particle composition. Realistic aerosols are difficult to describe and model, and yet attenuation by aerosols is often the limiting factor in IR detection, especially at low altitudes where aerosols are concentrated. When ASDIR was composed no provisions were made to compute attenuation by aerosols. While the program gives good results (as compared against actual measurements) at high altitudes and high latitudes, its predictions at lower altitudes are unrealistic.

LOWTRAN, another large computer program developed by the Air Force Geophysics Laboratory, predicts atmospheric

IR transmission over the spectral range from 0.25 to 28.5 μm . LOWTRAN computes attenuation by all the major atmospheric constituents and even by several of the trace gases in air. The latest edition of LOWTRAN includes five aerosol models and makes provision for the user to insert his own aerosol model if desired. LOWTRAN is the most widely distributed transmission code and has become a standard in the field of atmospheric propagation studies.

Objectives

The objectives of this independent study are to write an aerosol subroutine, based on the physics of LOWTRAN, for insertion into the ASDIR code and to investigate the attenuation of IR radiation by atmospheric aerosols. A minor modification to the LOWTRAN logic is made to account for results from a recent attenuation study at Grafenwohr, Federal Republic of Germany.

Approach

LOWTRAN parameters needed to predict aerosol transmission are (1) assumed aerosol particle densities (2) equivalent sea level path lengths for vertical paths, $AV(z)$ and (3) total sea level extinction coefficients for the "average continental" and "maritime" aerosol models. For this study, curve fits were obtained for these parameters giving analytical expressions which are easy and efficient for use in the large ASDIR computer code.

Using the curve fit results, a subroutine called HAZE

was written which computes the aerosol transmission as a function of wavelength, meteorological range, altitudes, and slant range for either of two selected aerosol models. The subroutine was validated against LOWTRAN and installed into ASDIR. Several runs of the modified ASDIR program were made using an assumed black body "target" at a given temperature and range. The total transmission curves produced by the modified ASDIR were compared against similar predictions from LOWTRAN to validate the installation of the HAZE subroutine into ASDIR.

Assumptions

Several specific assumptions that should be mentioned here are:

(1) The aerosol extinction coefficients used in LOWTRAN result from Mie theory calculations which assume the particles are monodispersed, homogeneous spherical particles. Most real aerosols consist of nonspherical particles.

(2) LOWTRAN particle densities are characteristic of only a few real atmospheres. Actual densities at any location may vary considerably from the LOWTRAN distributions because of local aerosol production mechanisms (eg. factories, desert sand, ocean, etc.)

(3) Beer's Law is used in this study to compute the transmission of energy in a narrow waveband (typically 20 cm^{-1}). The law holds exactly only at a single

(monochromatic) wavelength. Here, an average extinction coefficient over the small waveband is used to decrease the running times of the computer programs. Higher accuracy can be achieved by decreasing the wavelength interval but with a corresponding increase in cost.

Development of the Report

In Chapter II a brief description of the ASDIR emission program is given to further define its purpose, methodology, and its need for an aerosol prediction capability. Next, a general treatment of atmospheric aerosols is given with emphasis on the quantities used by the LOWTRAN aerosol predictive scheme. A brief section on the theory of IR extinction follows in which Beer's Law is defined along with the relationship between meteorological range and particulate density. Chapter II closes with a brief discussion of LOWTRAN, again with emphasis on its aerosol attenuation prediction scheme. The development of the subroutine HAZE for inclusion into ASDIR is described in Chapter III. Results of the systematic curve fits of extinction coefficients, particle densities, and aerosol equivalent path lengths are listed. Results of the subroutine HAZE calculations are presented in plots and compared against LOWTRAN results for similar cases. Chapter III also discusses the results obtained with the modified ASDIR program and the value of an aerosol

computation capability. Comparisons are given between modified ASDIR and LOWTRAN results for a few cases. Limitations of the modified ASDIR program are discussed along with recommendations for future development of the ASDIR code.

II. Background and Theory

ASDIR - IR Emission Prediction Program

The Aeronautical Systems Division's Infra-Red Emission Prediction Model (ASDIR) was developed in 1972-74 and is documented in three volumes (Stone and Tate, 1975a, b, c) available through the Defense Documentation Center (DDC). ASDIR is a composition of programs that compute the IR energy emitted by the airframe, engine, and plume of an aircraft in flight.

Infrared energy is constantly being emitted by all objects. In a complex object such as an aircraft in flight important emitters are:

- (1) hot parts of engine exhaust systems
- (2) hot gases of engine exhaust (plume)
- (3) aerodynamically heated leading edges and surfaces
- (4) heat exchangers
- (5) aircraft lights

In addition, background radiation from earth, sky, clouds, etc., and reflection of sunlight may be very important at certain viewing aspects and in certain wavelength bands. Figure 1 shows pictorially the various sources of IR radiation emanating from an aircraft.

The energy radiated (or reflected) from an aircraft will consist of both gray-body continuum radiation and molecular species (line spectra) radiation from the plume. IR emissions of a subject aircraft are summed from external

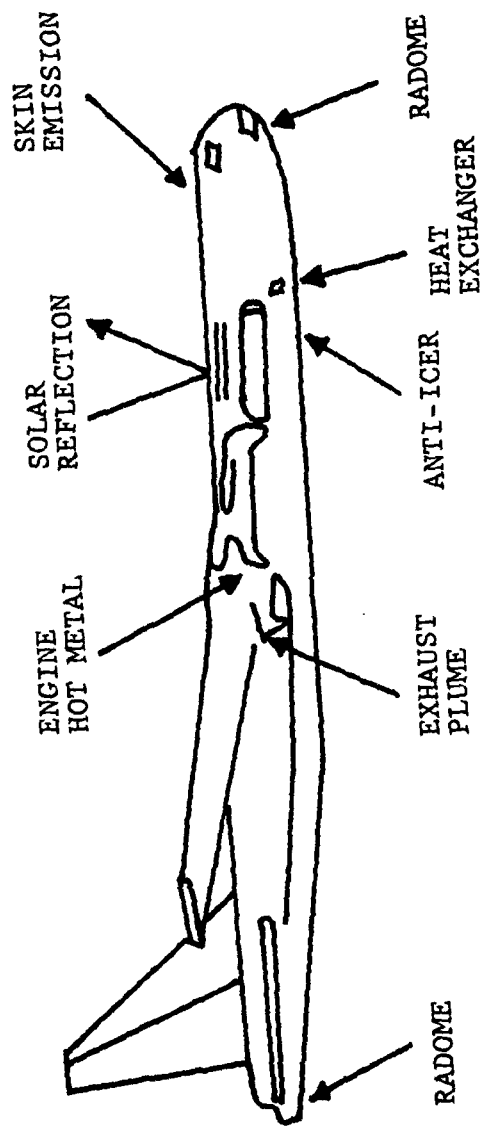


Figure 1. Aircraft IR Radiation Sources

surface and plume calculations over the frequency spectra. The summed emissions are presented as aspect distributions in azimuth and elevation of IR energy emitted from the aircraft and transmitted through the atmosphere to an observer at various ranges. The relative importance of the various contributors to the IR signature is shown in Fig 2. ASDIR's treatment of each of the main energy contributors and the atmospheric transmission scheme will now be considered.

Hot Surface Emissions. ASDIR uses a subroutine, SIGNIR, to predict IR emissions from axisymmetric turbojet, turbofan, and turboshaft engine exhaust system hot surfaces. SIGNIR, a product of the Vought Aeronautics Company, conducts an internal flow analysis, includes special surface cooling effects, and computes a thermal balance to provide the system surface temperature distribution (Stone and Tate, 1975c:2). The routine then calculates surface radiation (with multiple surface reflections) which emanates from the nozzle exit of the engine. The radiant energy is calculated in 10 to 25 wavenumber increments (wavebands) for IR wavelengths from 0.9 μm to 200 μm .

A flowchart for SIGNIR is shown as Fig 3. Inputs to the routine include the emissive properties of the metallic surfaces and the relative physical dimensions of engine exhaust system components. After a one-dimensional compressible flow analysis is performed, boundary layer calculations are made to obtain coefficients of convection and

Aircraft	Approach Hemisphere	Engine Mode	Low Wavelength Missiles						High Wavelength Missiles									
			Engine Contributors			Airframe Contributors			Engine Contributors			Airframe Contributors						
			Metal Emissions	Surface Reflections	Plume Emissions(3)	Airframe Emissions	Airframe Reflections	Metal Emissions	Surface Reflections	Plume Emissions(3)	Metal Emissions	Surface Reflections	Airframe Reflections					
Fighter/Interceptor (1)	Alt	Cruise Military Maximum	P	S	S	S	S	S	S	S	P	S	S	S	S	S	S	
	Forward	Cruise Military Maximum	S	S	S	S	S	S	S	S	S	S	S	S	S	S	S	S
Bomber (1)	Alt	Cruise Military Maximum	P	S	S	S	S	S	S	S	P	S	S	S	S	S	S	S
	Forward	Cruise Military Maximum	S	S	S	S	S	S	S	S	S	S	S	S	S	S	S	S
Helicopter (1)	Alt	Cruise Military	P	S	S	S	S	S	S	S	P	S	S	S	S	S	S	S
	Forward	Cruise Military	S(4)	S	S	S	S	S	S	S	S(4)	S	S	S	S	S	S	S
Fighter/Suppressed Engines (2)	Alt	Military	P	P	S	S	S	S	S	S	P	S	S	S	S	S	S	S
	Forward	Military	S	S	S	S	S	S	S	S	S	S	S	S	S	S	S	S
Bomber/Suppressed Engines (2)	Alt	Military	P	P	S	S	S	S	S	S	P	S	S	S	S	S	S	S
	Forward	Military	S	S	S	S	S	S	S	S	S	S	S	S	S	S	S	S
Helicopter/Suppressed Engines (2)	Alt	Military	P	P	S	S	S	S	S	S	P	S	S	S	S	S	S	S
	Forward	Military	S	S	S	S	S	S	S	S	S	S	S	S	S	S	S	S

(3) - Engine Plume Contribution Depends on Cycle - Turbojet Cycle Depicted Here.
(4) - Engine Installation is Controlling Factor - Assumed Straight Alt Exhaust Installation.

Notes: P - Prime Contribution
S - Secondary Contribution
(1) - Assumes Unsuppressed Engines
(2) - Assumes Suppressed Metal Emissions

Figure 2. Relative Importance of Contributions to a Weapon Systems Infrared Signature (Ref JTCC/AS Handbook, 1977)

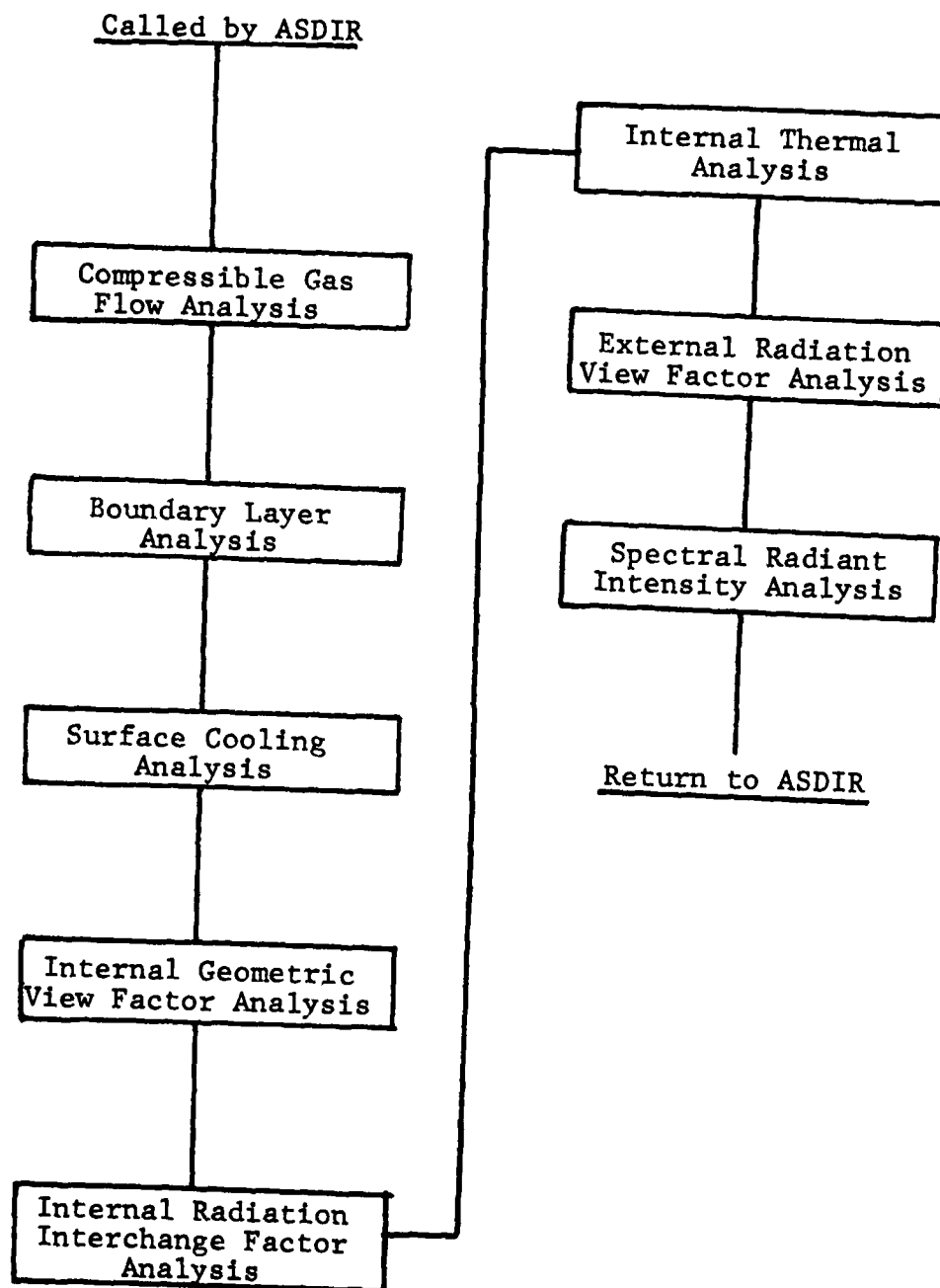


Figure 3. SIGNIR Flowchart as Used in ASDIR
 (Ref. Stone and Tate, 1975c:3)

friction along each surface in the system. Next, any cooling effects are considered such as transpiration, film or convection-film methods. Internal geometric view factors are then calculated which take advantage of symmetry and account for shadowing when the view between points is obscured by another surface.

After the geometric view factors are computed, and with surface emissivities available as input data, an overall radiation exchange factor is calculated. This factor, used in the radiation calculations, accounts for the view between two surfaces, the non-black nature of the surfaces and the multiple reflections occurring between all surfaces. The procedure assumes that all the emitting surfaces are Lambertian.

SIGNIR performs an internal heat balance on the system which considers radiation, convection and conduction. This balance provides the temperature at each of the internal surface nodes of the exhaust system for the calculation of the hot parts energy radiating from the exit of the engine exhaust. The radiant energy from the internal engine hot parts is considered to represent the background energy for those "rays" which emit to the observer from the engine nozzle exit. (See plume discussion for energy attenuated by the plume gases).

External Surface Emissions. External surfaces of the aircraft are treated as independent surfaces which occlude background incident energy and present their own grey-body

Lambertian energy. Each of an array of up to 20 surfaces is characterized by area, temperature, and emissivity. This array is prepared separately and provided to the ASDIR program as input. This treatment represents all external aircraft surface emitters such as aerodynamically heated or cooled regions (heat exchangers and exhaust ducts), lights, and even sun glint spots.

Plume Emissions and Atmospheric Attenuation. These two apparently independent quantities are discussed as if they were common because they are treated together within ASDIR. A subroutine (PLUSIG) treats the gaseous emission and absorption of molecular species, accounts for line broadening due to pressure and optical depth, and is designed to process these calculations over a wide range of temperatures. The calculation procedure for PLUSIG was worked out between Dr. G. Lindquist of The University of Michigan and Dr. C. Stone of ASD.

Background energy is treated as entering the plume "ray" from a point away from the observer and contributes to the energy after absorption in the plume gases. Should the background energy not be fully attenuated (absorbed) in passing through the plume, the plume appears as transparent. This transparency is most prominent for those plume rays which emit from the engine exhaust nozzle.

Plume rays are laid out on a geometrical basis taking advantage of axisymmetric symmetry (See Fig 4 for plume ray geometry). The origin of the ray geometry is the center of

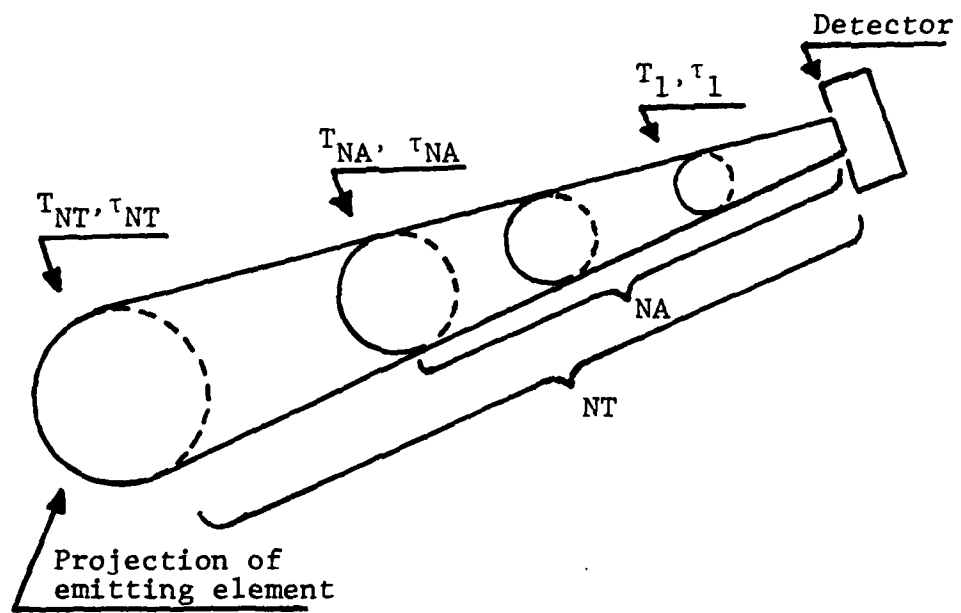


Figure 4. ASDIR Ray Geometry

the engine exhaust nozzle exit. Rays are divided into NT segments, NA of which are atmospheric. ASDIR uses a parallel ray assumption (treating the aircraft as a point source) which was a simplifying approximation of greater benefit to the treatment than the loss of accuracy it invokes. This consideration was based on included angles and relative ranges of intended typical problems.

From this short discussion it can be appreciated that the calculation procedure is complex and lengthy in view of the highly dependent nature of plume radiation on gaseous species concentration and distribution in the plume, the plume geometry, and absorption-emission physics of the plume gases. The general approach to the problem taken by PLUSIG is a gas band model based on the Curtis-Godson approximation. This technique is described in some detail by Goody (1964:236ff) and involves assigning to a non-homogeneous path (such as encountered in the plume) a temperature-scaled amount of absorbing matter at a mean pressure. A single spectral line absorbing along a non-homogeneous path can then be simulated by a line absorbing along a homogeneous path with both the intensity and width of the line empirically varied. Band parameters of line intensity, widths, and separations of the lines are functions of both wavelength and temperature for band models which both emit and absorb. These band parameters were experimentally determined in the laboratory from absorption measurements in isothermal samples of gas. Their use in a

computer code involves an array of the band parameters which are adjusted to approximate a homogeneous segment of gas in a plume. For the (assumed) homogeneous segment of gas the Planck emission law is then used to calculate its radiant energy.

PLUSIG divides the total path through the plume to the observer into NT segments, NA of them atmospheric as shown in Fig 4. Each of the NT segments along a ray is described by the gaseous partial pressures, temperatures, and length. The transmittance of each ray segment is computed by PLUSIG using several other subroutines. In the atmospheric segments PLUSIG includes only molecular H_2O , CO_2 , and N_2O as absorbing gases excluding aerosol effects. Work in this independent study was directed toward providing the capability to include aerosol attenuation in the atmospheric transmittance calculations of PLUSIG in the ASDIR program.

Specifically, a subroutine named ATMOS is addressed by PLUSIG which calculates the transmittances (τ_i 's) for each of the NA atmospheric segments along a ray from the subject aircraft to an observer. Using the methodology developed in LOWTRAN and described in Chapter II of this report, a subroutine was written which is called by ATMOS for modification of the atmospheric transmittances as necessary to account for aerosol extinction. Extinction represents scattered energy as well as energy absorbed by the aerosol particles. The total transmittance is taken as the simple multiple of the value computed without aerosol extinction

and the value computed by the new subroutine for each wavenumber-band.

Atmospheric Aerosols

The atmospheric air is never free of particles having a wide variety of origins, sizes, and chemical compositions. These particles constitute two main categories: (1) non-hygroscopic particles such as dust, volcanic ash, and even interplanetary debris and (2) hygroscopic particles that readily absorb and combine with water such as salt, hydrocarbons exuded by foliage, and many products of combustion. Collectively these suspended particles are referred to as aerosols. If we neglect clouds, rain, and fog droplets (i.e. visible water) and consider only the aerosols suspended in "dry" air, the term "haze" aerosol emphasizes the particulate nature of these efficient scatterers of infrared energy. Haze occurs in greatest concentrations near the earth's surface by virtue of relatively high molecular weight and is usually the determining factor of visibility (McCartney, 1976:114). Additionally, and of prime importance in this study, haze particles constitute an important source of IR attenuation throughout a wide spectrum of wavelengths. Thus, mathematical modeling of haze formations and prediction of haze attenuation are critical elements in estimating atmospheric transmission of radiant energy through "real-world" atmospheres.

The following sections provide a basis for the

theoretical treatment of haze attenuation which follows. Here are discussed sources of haze aerosols and particle composition, particle removal processes, particle size and size distributions, the complex index of refraction of haze aerosols, and the aerosol vertical distributions developed for use in the LOWTRAN transmission mathematical model.

Sources of Atmospheric Aerosols. Particles in the atmosphere are formed by a variety of processes some of which are man-made and others strictly natural phenomena. In some cases it is difficult and perhaps rather arbitrary to try to distinguish between the source types. Cadle (1966:7) classifies the formation mechanisms into five main groups:

(1) Condensation of vapor and sublimation of solids and the formation of smoke by both natural and man-made processes.

(2) Chemical reactions involving trace gases in the atmosphere.

(3) Mechanical disruptions and dispersal of matter from the earth's surface (includes sea salt over the ocean and various dusts over the continents).

(4) Coagulation of fine particles to form larger particles of mixed composition.

(5) Influx of interplanetary debris.

The diverse sources of haze aerosols produce widely differing sizes and concentrations of particles which are highly dependent upon the local conditions (eg. urban,

rural, or maritime locales) and consequently extremely complex to empirically represent. An additional complication is induced by the great variation in the attenuation effects from hygroscopic to non-hygroscopic particles. The models generally encountered in the literature usually empirically describe the aerosol concentrations as a specified sum of percentages of dry and hygroscopic particles.

Dust-Like (Non-Hygroscopic) Particles. Dust-like particles are continually being placed in the atmosphere by several processes. As the earth sweeps through space, interplanetary debris that range in size from small meteorites up to several tons may partially disintegrate upon entering the atmosphere and shower the earth's surface with millions of small particles.

Volcanoes inject ash and soot into the atmosphere, sometimes with spectacular results. McCartney (1976:116) comments that the eruption of Krakatoa in 1883 raised clouds of ash to 90,000 ft and completely darkened the skies for 100 miles. Within a few weeks the smaller particles from the eruption had completely circled the globe at high altitudes and produced unusual visual effects at sunrise and sunset for several years.

Soil dust blown into the atmosphere by the sculpting and lifting forces of winds of even moderate speed may often be transported great distances by atmospheric winds aloft. Forest fires are prolific manufacturers of aerosol haze particles some of which are non-hygroscopic.

Cadle (1966:12) estimated that an ordinary grass fire covering only one acre yields 2×10^{22} fine particles ranging in composition from inorganic ash to complex tars and resin. If all of those particles were distributed uniformly over the acre to an altitude of 10,000 ft the resulting concentration would be about $2 \times 10^9 \text{ cm}^{-3}$. As in the case of volcanic ash and desert dust, the residue of fires may travel great distances in the atmosphere.

Of ever-increasing importance is the injection into the air of many types of industrial products. Grating, blasting, smelting and other operations produce several forms of dust-like particles which vary greatly in size and number density. The larger particles quickly settle back to earth while the smaller (radius $< 1.0 \text{ } \mu\text{m}$) move with winds and remain suspended until removed by one of the processes of atmospheric scrubbing described in a later section.

Hygroscopic Particles. The most significant type of hygroscopic particle in the atmosphere is sea salt composed mainly of sodium chloride. The importance of sea salt particles results from their being so numerous; they are widespread over both oceans and continental areas. Besides being a consideration in radiant energy attenuation, sea salt particles also play a role as nuclei in cloud formation. Byers (1965:70) reports that a nucleus of NaCl of 10^{-9} gm dry mass (approximately $5 \text{ } \mu\text{m}$ equivalent spherical radius) becomes a water drop of $25 \text{ } \mu\text{m}$ radius at a relative humidity of 99 per cent. Thus, sea salt particles in the

atmosphere present extreme complexities in aerosol modeling by their growth capability and subsequent changes in attenuation effects.

It has been established, as reported by McCartney (1976:119), Cadle (1966:8) and others, that sea salt particles are mainly formed by the bursting of air bubbles as they reach the surface of the sea. These droplets, after evaporation, produce particles with an effective radius of 0.15-1.15 μm . The smaller salt particles are then caught up by the wind, carried aloft and can be transported great distances. This explains why several researchers estimate the aerosol composition in central Europe (500 miles inland) to be 70-80 per cent maritime (largely sea salt) and 20-30 per cent continental (dust-like) particles.

There are many man-made sources of hygroscopic aerosol particles. Several types of particles are produced by photochemical reactions and nucleations between combustion gases and atmospheric trace gases. For example, sulfur dioxide, a result of the combustion of coal and petroleum derivatives, is oxidized by solar photosynthesis to form sulfuric trioxide. These particles are very hygroscopic, form sulfuric acid, and can become extremely corrosive. Other materials such as nitrogen dioxide (from automobile exhausts), hydrogen sulfide and other sulfate particles abound in the atmosphere.

Particle Removal Processes. The particles being placed in the atmosphere from the sources previously

described are continually being removed or scrubbed by several removal processes. These must be briefly discussed so that an understanding of the dynamic nature of atmospheric aerosol content may be achieved.

The simplest removal process is that of gravity which causes fall-out or sedimentation of the particles. This process is quite important since it controls somewhat the upper limit of aerosol particle sizes (Junge, 1962:123). In settling through still air a particle will obtain a terminal velocity when the gravitational force is balanced by viscous drag. The viscous drag is a function of air density, so that a particle having an appreciable fall speed at a height of 80 km may essentially float at 20 km. Sedimentation may sometimes result in concentrations in specific layers, especially when the particles are out of reach of rain which causes "washout".

Washout is the removal of particles by precipitation and is very effective in clearing the air. Washout implies some kind of interaction (joining) between the precipitation droplet and the aerosol particle. Actual physical contact between the two may not be necessary and, in fact, aerosol particles are known to be carried around raindrops in the associated airstream (Byers, 1965:76).

Coagulation is a third removal process and occurs when two particles collide and coalesce, resulting in fewer but larger particles. The general theory for coagulation is founded on a statement of the rate of collisions of

particles as they diffuse through the air by Brownian or turbulent motion. An interesting result of the theory (see Junge, 1963 for a detailed treatment) is that the concentration of smaller (Aitken) particles is decreased very rapidly by coagulation as compared to the larger particles. This fact helps to fix the practical lower limit of aerosol particle sizes in "well-developed" atmospheres. A more detailed treatment of aerosol sizes and distributions is presented in a later section of this chapter.

Particle Composition. It is apparent from the previous discussions that a wide diversity exists in sources of aerosol particles and thus in particle composition. It is therefore an extremely difficult task to estimate the particle composition, size distribution, and number density of aerosols in any particular application. On the other hand, aerosol chemical composition is very important in determining the complex refractive index for use in Mie theory calculations of scattering and absorption coefficients. Many investigations have sought to determine the compositions of aerosols and the combined effects of the production and removal processes. These investigations have been seriously hampered by the difficult task of measuring the composition of the very small (Aitken) particles. While the approximate concentrations of Aitken nuclei can be determined by such means as the Aitken counter (similar to a Wilson cloud chamber) exact compositions of these particles remain an open question. However, observations

of the aggregate behavior of Aitken particles (eg. growth curves) infer that their chemical composition is similar to large or giant particles and mainly of continental origin (Junge, 1963:157).

In summary, the constitution of aerosol particles in the atmosphere varies between two extremes: dry insoluble dust particles and completely soluble (hygroscopic) materials. Additionally, any specific particle is changing in time under the influence of coalescence, coagulation, and combination with atmospheric gases. These facts lead to the simplifying step of treating the atmosphere by using a mixed particle concept. This concept assigns an average composition and average index of refraction to the entire distribution of particles. The value of this concept in applications is obvious; it limits having to determine an explicit aerosol distribution for each particle of differing composition. The mixed particle concept is employed in LOWTRAN calculations of extinction coefficients and thus represents a primary assumption in the analysis adapted for this thesis.

Particle Sizes. An understanding of the variety of aerosol production and removal mechanisms has been established, so it is seen that, just as the particle compositions vary greatly, so does the range of particle sizes. For most applications in IR engineering, particles must be considered whose radii extend over nearly four orders of magnitude. Figure 5 adapted from Junge (1963:112) shows

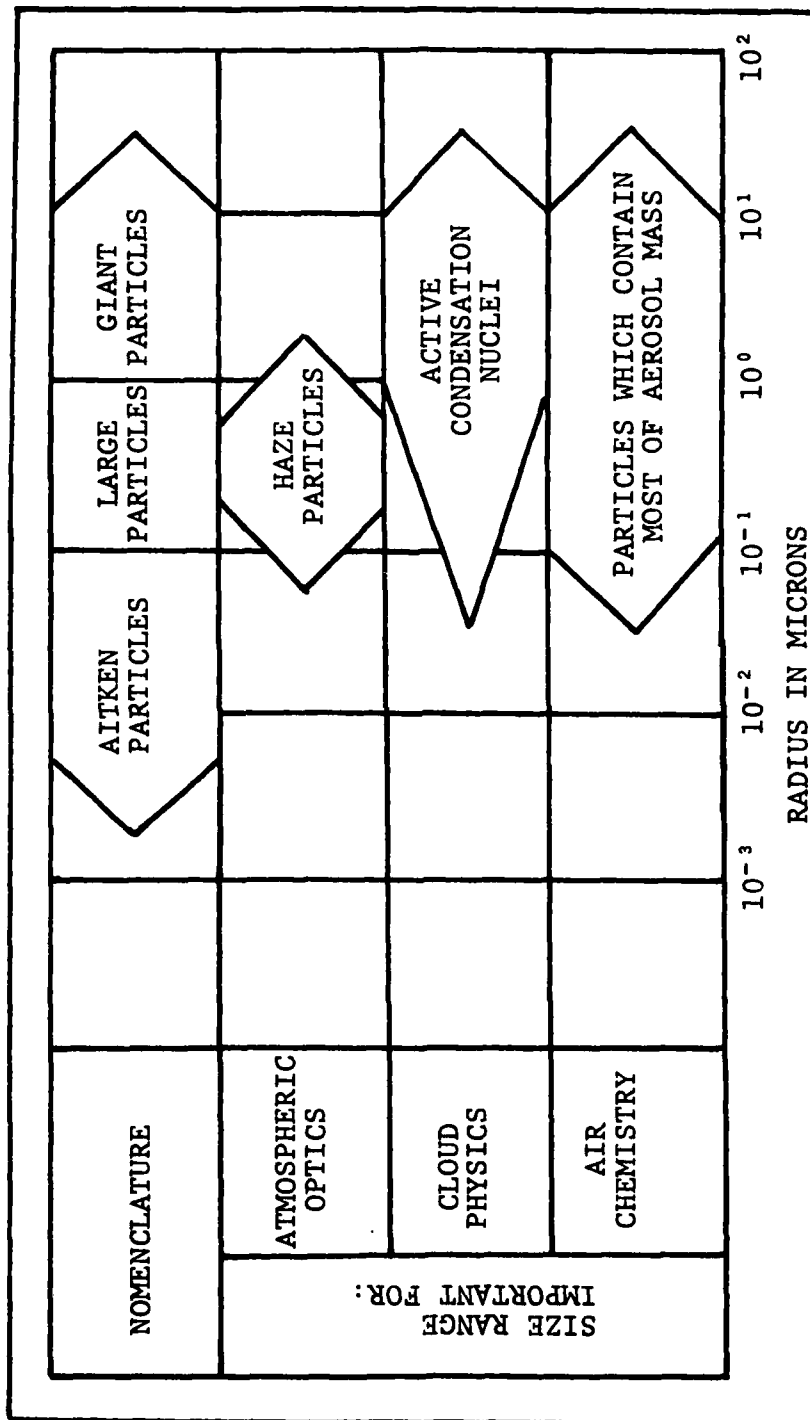


Figure 5. Size Ranges of Aerosols
(Ref Junge, 1963)

both the nomenclature and importance of particle sizes for the various fields of atmospheric science. Of special interest in this thesis are:

Aitken particles	$0.02 < r < 0.1 \text{ } \mu\text{m}$
Large particles	$0.10 < r < 1.0 \text{ } \mu\text{m}$
Giant particles	$1.00 < r < 100 \text{ } \mu\text{m}$

The various cutoffs in the particle radii are not arbitrary but are based on many measurements which yielded surprisingly similar results.

The primary factor that determines the lower limit of particle radii is the rate of coagulation of the very smallest particles (Byers, 1965:72). Junge (1963:130) calculated the effects of coagulation and "aging" on a sample haze aerosol. Figure 6 shows how the concentration of the small Aitken particles decreases very rapidly compared to the time scale of other meteorological processes. The figure shows that in natural aerosols the effects of coagulation are such that the maximum of the distribution falls between 0.01 and 0.1 μm . This occurs because particles smaller than 0.005 μm can exist only briefly causing any maximum below 0.01 μm to rapidly disappear.

On the large end of the particle spectrum, sedimentation due to gravity is the controlling factor in limiting the upper radius. Junge (1963:123ff) used general diffusion theory to predict that particles of radius greater than 20 μm would quickly settle back to earth under normal conditions. He also summarized results of several

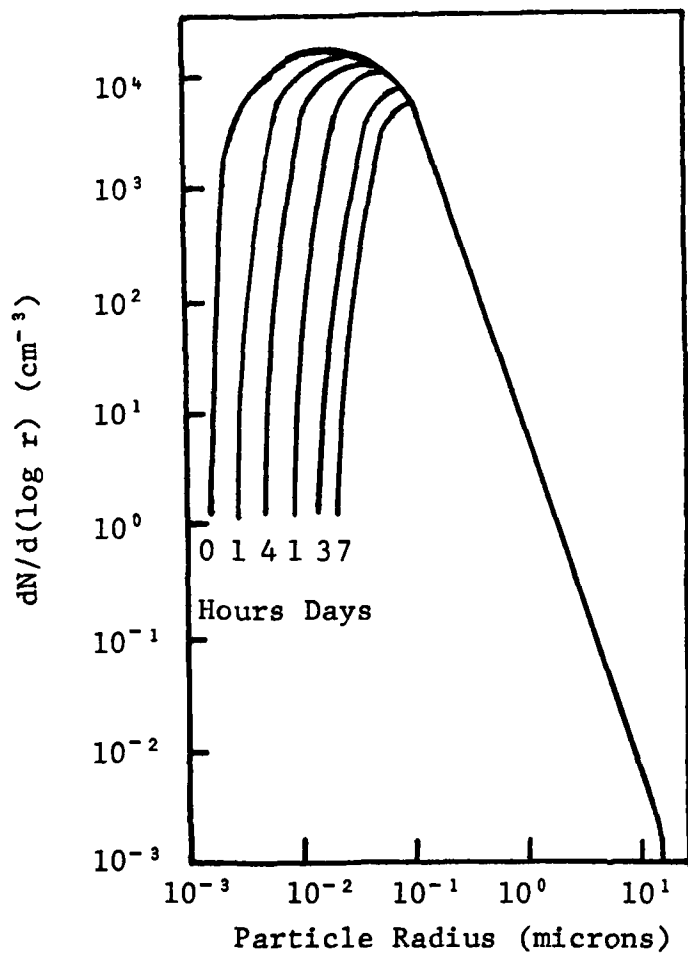


Figure 6. Size Distribution of Aerosol Particles with Coagulation Affecting the Lower Size Range (Ref Junge, 1963)

investigations which showed that indeed the measured maximum cutoff was consistently between 10-20 μm . Even over the oceans, where particles larger than 20 μm radius are continually injected into the air by bursting air bubbles, the 20 μm cutoff was still observed. LOWTRAN's use of 0.1 μm and 100 μm as lower and upper particle size limits appears well justified by experience.

Within the well-established limits of particle size radii it is possible to make some general comments concerning the sizes of particles of different compositions. Dusts, smokes, and dry haze which produce the principal optical scattering in the atmosphere usually have radii between 0.1 and 1.0 μm (Byers, 1965:70). Scattering by these small particles helps account for the blue tint of an otherwise clear sky. Sizes up to 100 μm or greater may occur in dust storms or in areas of industrial pollution but, as noted before, these larger particles rapidly settle out of the air. It has also been pointed out that hygroscopic particles, especially sea salt, can grow very rapidly with increases in relative humidity. Cadle (1966:9) points out that below about 75 per cent relative humidity sea salt/water droplets completely evaporate and leave particles about 1.25 μm in radius. The significance of that size is that these particles are small enough to be carried aloft by atmospheric winds and penetrate far inland. Thus, many locations in central Europe may be characterized by the continental/maritime particle mixes as mentioned earlier.

Measured Particle Size Distributions. An important characterization of any aerosol is its size distribution function which defines the manner in which the particle population is spread over the range of sizes. While it was once thought that natural aerosols consisted of fairly discrete groups of particles, recent improved instrumentation has shown that aerosols have essentially a continuous size distribution with well-established upper and lower limits of particle size. Thus, particle measurement investigations usually produce either histograms or continuous distribution curves in which the number of particles within a radius interval (Δr or dr) is represented by the area over that interval. Because of the wide range of particle sizes and concentrations, logarithmic scales are desired. The techniques used to count and measure particles provide data on the number of particles per specified radius interval (typically 0.1 or 0.2 μm in width). For very narrow size classes (Δr small) a continuous distribution may often be approximated.

For a continuous distribution the number of particles per unit interval of radius and per unit volume is

$$n(r) = \frac{dN}{dr} \quad (1)$$

where the differential quantity dN expresses the number of particles having a radius between r and $r+dr$, per unit volume according to the distribution function $n(r)$.

Formally, the total number of particles per unit volume is obtained by the integration:

$$N = \int_0^{\infty} n(r) dr \quad (2)$$

In practice, cutoff or limiting values of radii are used as limits instead of zero and infinity. Also, a cumulative concentration N_c may be defined as the number of particles with radii less than r by the equation

$$N_c = \int_{r_0}^r n(r) dr \quad (3)$$

where r_0 is the lower cutoff for particle radius. A particle distribution of this type is the basis of the aerosol attenuation calculations in LOWTRAN and is adapted for use in the modification to the ASDIR computer program.

A derivative of Eq 2 is often used in practice where a log radius number distribution is defined because of the wide range in particle sizes and concentrations. The log radius number distribution may be written as

$$n_L(r) = \frac{dN}{d(\log r)} \quad (\text{cm}^{-3}) \quad (4)$$

where N is again the total concentration (particles-cm⁻³) of aerosol particles with radii smaller than r . Attempts to describe particle size distributions have led to several

proposed analytical expressions to represent the aerosol environment.

A commonly-used distribution, first developed by Junge (1963) from experimental work performed on continental aerosols, may be written as a "power-law". Junge concluded that the particle size distribution for an "average continental aerosol" can be represented by an exponential curve (see Fig 7) of the form

$$n_L(r) = \frac{dN}{d(\log r)} = cr^{-b} \quad (5)$$

between $r=0.1 \mu\text{m}$ and $r=20 \mu\text{m}$. In Eq 5, c is an empirical constant whose value depends on the specific concentration and b is dependent on the distribution. While b is variable it has been found to be approximately 3 for most naturally-occurring aerosols (McCartney, 1976:141).

Equation 5 can be put in nonlogarithmic form by noting that

$$d(\log r) = 0.434 d(\ln r) \text{ and } d(\ln r) = \frac{dr}{r} \quad (6)$$

Thus, we can write

$$n(r) = \frac{dN}{dr} = 0.434 cr^{-(b+1)} \quad (7)$$

Of course, actual particle size distributions may vary considerably on an individual basis from the power-law approximation. However, distributions of the form given in

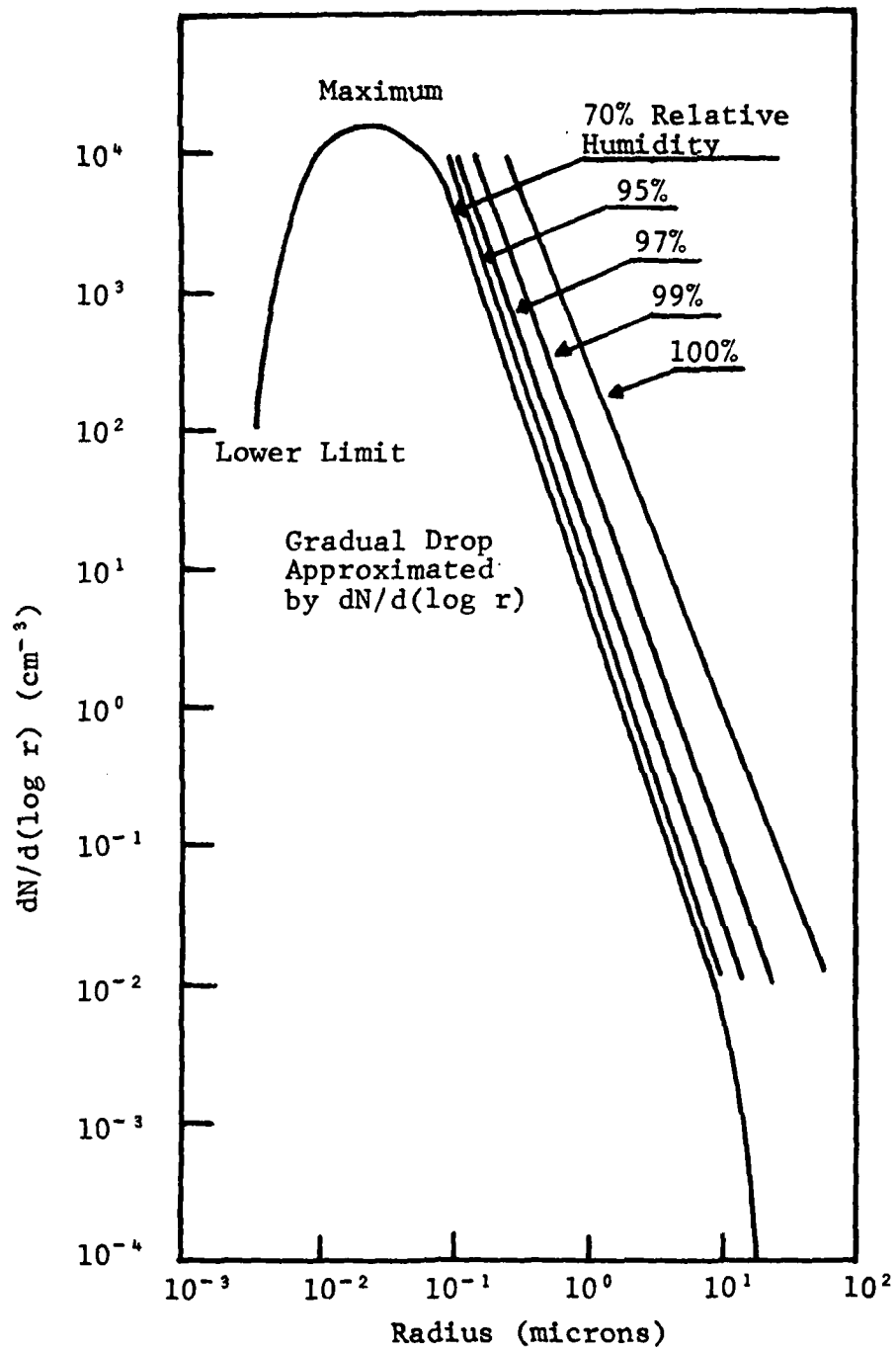


Figure 7. Average Size Distribution for Continental Aerosols Near the Earth's Surface (Ref Junge, 1963)

Eq 7 have been found by many independent investigators to be a good representation of aerosols having a wide variety of origins and compositions (McCartney, 1976:141). Both measured and deduced aerosol concentrations have been shown to agree quite well with the predicted power-law expressions.

Aerosol Vertical Distributions. For general applications, such as those for which ASDIR is used, one is interested in IR attenuation along slant paths between an emitter at one altitude and a detector at another. Thus, it is necessary to know how aerosol particle concentrations vary with altitude. This "vertical aerosol distribution" is affected by a number of factors, the most important of which is normally the size distribution at the surface. The local aerosol production mechanisms and the origin and history of the local air mass are also significant factors. Qualitatively, air layers over the land masses are the most polluted (naturally and artificially) in terms of aerosol particle concentrations. Most of this pollution is contained in a "mixing layer" that extends upward to 3-5 km and can be significantly affected by temperature and pressure profiles in the air layers.

The concept of the mixing (or boundary) layer is an important one in aerosol attenuation studies. The lowest levels of the atmosphere are well stirred by winds and convective currents, and the mixing ratio of aerosol particles is fairly constant in these layers. The mixing ratio

may be expressed either as the ratio of the total mass of particles to a unit mass of air, or as particle to molecular number density. Since the density of air decreases exponentially with altitude, the particle concentration should also decrease approximately exponentially with altitude. Penndorf (1954) analyzed data from many airborne measurements of the attenuation of solar flux and found that particle concentration showed the expected exponential decrease with altitude in the first 5 km above the surface. The LOWTRAN assumed particle distributions also show this exponential decrease in the lower 5 km. LOWTRAN's particle distributions will be adapted without change for the modification to ASDIR.

For an exponentially decreasing particle distribution the variance of particle concentration with altitude is

$$N_z = N_0 \exp(-Z/H_p) \quad (8)$$

where

N_0 = particle concentration (cm^{-3}) at ground level

H_p = scale height for the aerosol (ie. the altitude at which the concentration is $1/e$ times the ground level)

N_z = concentration (cm^{-3}) at an altitude z

Penndorf's data showed H_p to be between 1 and 1.4 km with 1.2 km being a good average.

Using Eq 8 one can define an equivalent sea level path length through the aerosol environment completely analogous

to the concept of equivalent paths for molecular absorption. The equivalent path length is simply the horizontal distance (at ground level) that has the same attenuation as the true (slant) path length. The concept lets one evaluate the amount of particles and the resulting attenuation in terms of a path length at sea level where the concentration is either known or can be estimated with reasonable accuracy. Figure 8 illustrates the geometry of slant paths in the plane parallel (flat earth) approximation. Using \bar{R} to denote the equivalent path length:

$$\bar{R} = H_p \sec\theta (\exp(-R_1 \cos\theta/H_p) - \exp(-R_2 \cos\theta/H_p)) \quad (9-a)$$

$$= H_p (R/Z_2 - Z_1) (\exp(-Z/H_p) - \exp(-Z_2/H_p)) \quad (9-b)$$

where

Z_1 = altitude of point #1

Z_2 = altitude of point #2

R = slant range between points #1 and #2

R_1 = slant range from sea level to point #1

R_2 = slant range from sea level to point #2

θ = zenith angle measured absolute from the local vertical

H_p = scale height for aerosol as in Eq 8

A word of caution is in order here because the above expression is developed using a "flat earth" approximation with a nominal restriction on zenith angles of about 75 deg. But at large zenith angles transmission is poor through any

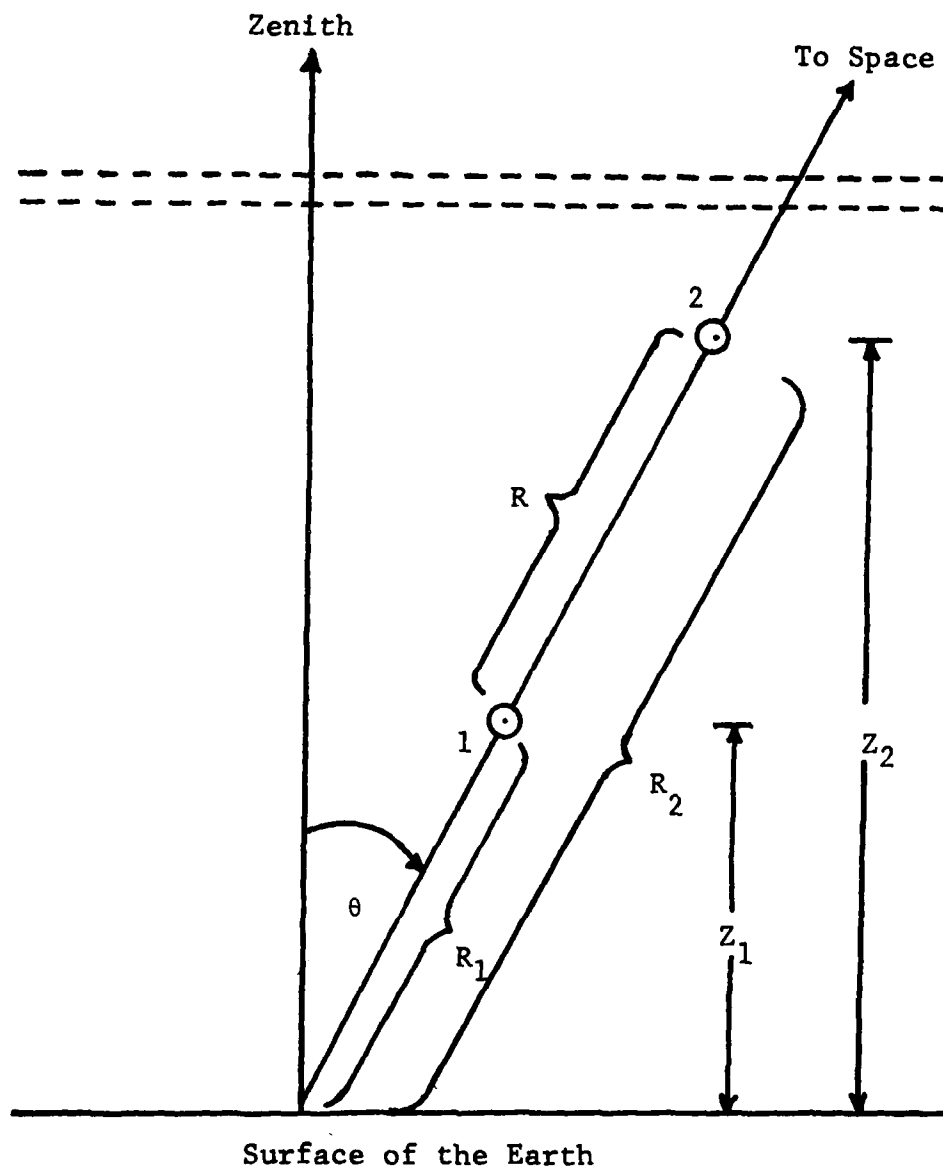


Figure 8. Geometry of Slant Paths in the Plane-Parallel Approximation for Calculating Equivalent Path Lengths

haze, and large geometric ranges are seldom involved. Thus a cautious use of Eqs 9 may be justified even for large angles.

With the factors discussed in this section taken into account, many workers have devised models of the vertical profiles of hazes found in real atmospheres. Using blends of measured particle concentrations, attenuation measurements and scattering theory, Elterman (1964) set up such a profile that has been widely used in subsequent modeling efforts. His profile was later revised (Elterman, 1968) to account for long-term stratospheric effects on aerosol distributions that were determined by new measurement techniques. Both models are shown in Fig 9. Note the exponential decrease in concentration from 200 cm^{-3} at sea level to about 0.02 cm^{-3} at 10 km for the 1964 model. A modification of Elterman's 1968 model was incorporated into LOWTRAN and is further described in a later section describing the LOWTRAN code.

Complex Index of Refraction. Since particles in the atmosphere have such a wide variety of chemical compositions, it is extremely difficult to determine the complex index of refraction of a real aerosol. The index of refraction is a complex number whose real part corresponds to scattering and whose imaginary part is used to compute absorption in Mie theory calculations. It is apparent that hygroscopic particles capable of rapid growth by combining

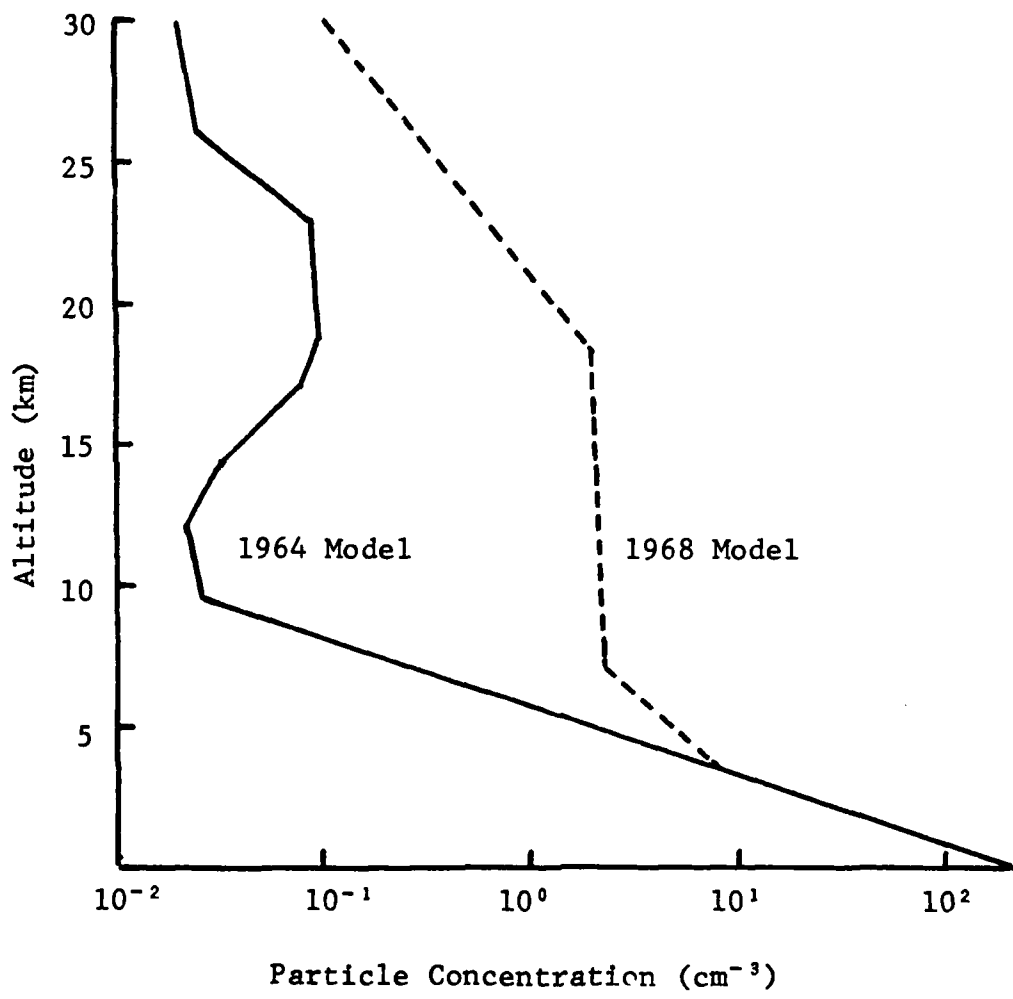


Figure 9. Vertical Profiles of Particle Concentration from Elterman (1964, 1968)

with water add to the complexity of determining the total index of refraction.

The real part of the index of refraction of common aerosols has been estimated at about 1.5 by several investigators, (Volz, 1972; Hanel, 1976) while the imaginary part, is less well-established. Fortunately, absorption by aerosols is usually small and the real part of the index of refraction is usually adequate to predict attenuation of the particles.

Volz (1972) computed tables of average refractive indices based on studies of typical distillates of rain-water. These values were used for computing aerosol extinction coefficients using Mie theory (Appendix A). The resulting extinction coefficients were used in the first LOWTRAN program. The original aerosol model in LOWTRAN was known as the "average continental model" and assumed the aerosols to be composed of 70 per cent water-soluble substances and 30 per cent dust-like substances. This model was considered typical of Central European environments. Later editions have included other model aerosols (eg. urban, rural, maritime) which differ primarily in the assumed mix of hygroscopic and non-hygroscopic particulates. The values tabulated by Volz and the extinction coefficients computed from them as used in LOWTRAN are adopted without change for use in this thesis.

Extinction of IR Energy in the Atmosphere

Atmospheric attenuation or extinction are terms used to express the processes by which electromagnetic energy is scattered and absorbed by the atmospheric constituents as that energy travels from an emitter to a sensor. The primary scatterers and absorbers in the atmosphere are the molecules of the air itself, water droplets in the form of fog and precipitation, and aerosols such as particulate haze. The fundamental premise of attenuation of energy is the Beer-Lambert law which states that the attenuation is dependent on the amount of matter along the path of the radiation. The law assumes that the physical state (temperature, pressure, composition) of the medium is uniform along the path. The monochromatic spectral transmission of optical radiation is then

$$\tau = I/I_0 = \exp(-\beta_T L) \quad (10)$$

where

τ = transmittance in per cent of original radiation propagated

I_0 = incident intensity of radiation

I = emerging intensity of radiation

β_T = total extinction coefficient

L = length of path traversed by the radiation

The total extinction coefficient β_T reflects both processes of scattering and absorption and may be written

as

$$\beta_T = \beta_{Sc} + \beta_{Ab} \quad (11)$$

where

β_{Sc} = total scattering coefficient

β_{Ab} = total absorption coefficient

The two coefficients above (β_{Sc} and β_{Ab}) may be further broken down into aerosol and molecular scattering and absorption coefficients as

$$\beta_{Sc} = \beta_{Sc/aero} + \beta_{Sc/mol} \quad (12-a)$$

$$\beta_{Ab} = \beta_{Ab/aero} + \beta_{Ab/mol} \quad (12-b)$$

and the total aerosol extinction coefficient may be written as

$$\beta_{aero} = \beta_{Sc/aero} + \beta_{Ab/aero} \quad (13)$$

The values of β_{aero} as a function of wavelength of incident radiation may be calculated by Mie theory as briefly outlined in Appendix A where β_{aero} is dependent upon the aerosol particle radius, the complex index of refraction of the particle, and the particle size distribution. As developed in Appendix A, the single most important factor in determining the aerosol extinction coefficient is the dimensionless size parameter α given by

$$\alpha = \frac{2r}{\lambda} \quad (14)$$

where

r = particle radius

λ = wavelength of incident radiation

Mie calculations show that absorption by most dust-like particulates is very small and can be reasonably neglected in most applications. Scattering by all aerosol particles, however, is a very important part of atmospheric attenuation and must be accounted for in some detail.

Considering the other factors in Eqs 12, scattering by the molecules of the air itself is significant at optical wavelengths and helps account for the blue tint of the sky. At wavelengths greater than 0.6 μm (which includes the IR portion of the spectrum) this scattering by the extremely small molecules becomes negligible compared to aerosol scattering (Rensch, 1968:1). Thus, molecular (also termed Rayleigh) scattering is safely omitted in the ASDIR program for the long wavelength applications.

Molecular absorption, denoted by $\beta_{\text{Ab/mol}}$ in Eq 12-b is an extremely complicated function that represents a major hurdle in computer prediction codes such as ASDIR and LOWTRAN. Both codes use a "waveband" model to calculate molecular absorption in very narrow wavelength bands for the major molecular attenuators. These attenuators in order of importance are: H_2O , CO_2 , O_3 , N_2O , CO , O_2 , CH_4 , and N_2 (McClatchey, et al, 1972:11). H_2O , CO_2 , and O_3 (in some narrow wavelength bands) are by far the most

important absorbers. Both LOWTRAN and ASDIR have demonstrated ability to calculate the absorption by molecular gases to a reasonable accuracy in most areas of the spectrum. Calculation of aerosol extinction, especially in the lowest layers of the atmosphere, is still a large uncertainty in LOWTRAN and has been, as noted, nonexistent in ASDIR.

Aerosol Extinction. The discussion thus far of the physical production mechanisms of aerosols qualitatively suggested the importance of aerosols as attenuators of electromagnetic energy. This section will treat the total extinction due to aerosols as predicted by Mie theory. The essence of this section is the use of the extinction coefficients predicted by Mie theory and the connection between certain meteorological parameters and aerosol extinction.

Mie theory predicts an extinction coefficient for spherical polydispersed particles as (Rensch, 1964:4)

$$\beta_{\text{ext}} = \pi \int_{r_1}^{r_2} Q_{\text{ext}}(m,r)n(r)r^2 dr \quad (15)$$

where

- $n(r)$ = the size distribution of the spheres
- $Q_{\text{ext}}(m,r)$ = extinction efficiency at radius r
(See Eq 45)
- r = particle radius
- m = complex index of refraction of the particle
- r_1, r_2 = lower and upper limits of the aerosol distribution

Assuming a size distribution as suggested by Junge and given by Eq 7, substitution into Eq 15 gives

$$\beta_{\text{aero}} = 0.434c\pi \int_{r_1}^{r_2} Q_{\text{ext}}(m,r)r^{1-b}dr \quad (16)$$

Changing the independent variable to $\alpha=2\pi r/\lambda$ converts Eq 16 to the following:

$$\beta_{\text{aero}} = 0.434c\pi \left(\frac{2\pi}{\lambda}\right)^{b-2} \int_{\alpha_1}^{\alpha_2} \frac{Q_{\text{ext}}}{\alpha^{b-1}} d\alpha \quad (17)$$

$$= 0.434c\pi \left(\frac{2\pi}{\lambda}\right)^{b-2} K \quad (18)$$

where

$$K = \int_{\alpha_1}^{\alpha_2} \frac{Q_{\text{ext}}}{\alpha^{b-1}} d\alpha \quad (19)$$

The role of the constant c in Eq 17 needs closer examination. From Eq 7 it is seen that the dimensions of c are $(\text{length})^{b-3}$ and the value of c depends on the particle concentration. Rearranging Eq 17 shows that

$$c = 2.304 \left(\frac{\lambda}{2\pi}\right)^{b-2} \frac{\beta_{\text{aero}}}{\pi K} \quad (20)$$

Next, a well-established relation between meteorological range and the extinction due to aerosols and air molecules at $\lambda=0.55 \mu\text{m}$ is the Koschmeider equation (McCartney, 1976:42)

$$R_m = \frac{1}{\beta_{Sc}} \ln\left(\frac{1}{T}\right) = \frac{3.91}{\beta_{Sc}} \quad (21)$$

where absorption in the visual wavelengths is neglected and T , the observer's visual contrast threshold is taken as 0.02. The above equation largely eliminates the subjective factors present in many operative definitions of visibility. R_m is obtained by specifying that distance at which a large black object can be seen against a day sky background with $T=0.02$. The value for T has been validated by several independent researchers as being appropriately average. β_{Sc} is approximately equal to the total spectral extinction coefficient at $0.55 \mu\text{m}$ which is due primarily to scattering by both aerosols and the molecules of the air. The value of $\lambda=0.55 \mu\text{m}$ is used as the wavelength of greatest sensitivity of the human eye. Equation 21 may then be written as

$$\beta_{aero}(0.55 \mu\text{m}) = \frac{3.91}{R_m(0.55 \mu\text{m})} - \beta_{mol}(0.55 \mu\text{m}) \quad (22)$$

where the terms in parentheses indicate that meteorological range refers to a specific wavelength of $0.55 \mu\text{m}$.

Mie theory establishes that the aerosol extinction coefficient β_{aero} is directly proportional to the aerosol number density $N(z)$ so we can write

$$N(z) = \frac{a(z)}{R_m} + b(z) \quad (23)$$

where $a(z)$ and $b(z)$ are constants for any given altitude z . The above equation can be used, as it is in LOWTRAN, to interpolate/extrapolate to visual ranges other than those for which specific values of $N(z)$ are given as in Table 1 for visual ranges of 5 km and 23 km. A later section in this chapter discusses further the use of this procedure in LOWTRAN which is adapted for use in ASDIR.

LOWTRAN-AFGL Transmission Model

The most widely-accepted computer model in use for predicting atmospheric transmittances is LOWTRAN, under constant development and improvement by the Air Force Geophysics Laboratory (AFGL). LOWTRAN is an evolutionary product (LOWTRAN 4 is the latest edition) that is updated as new data concerning molecular and aerosol effects are generated. The program is "user oriented" in that it is well documented, easy to operate, and thus well suited for field use. No attempt here is made to fully describe the LOWTRAN methodology, but the interested reader is referred to McClatchey, et al (1972); Selby and McClatchey (1972, 1975); and Selby, et al (1976, 1978) for a complete

background description and documentation of the program. Especially useful is Optical Properties of the Atmosphere by McClatchey, et al (1972) in which the theoretical basis for the LOWTRAN program is fully outlined with exception of the current aerosol treatment. Here only a brief description of the program will be given with particular emphasis on the aerosol attenuation method.

LOWTRAN-A General Description. LOWTRAN computes the transmittance of the atmosphere over a broad wavelength interval with wave number spectral resolution of 20 cm^{-1} (waves per cm). It falls into the general category of wave band model schemes and is based on laboratory transmittance measurements complemented by emission line theory molecular constants compiled and presented by McClatchey, et al (1972). The program is capable of predicting transmittance along arbitrary slant paths in the wavelength region 0.25 to $28.5 \mu\text{m}$ (ultraviolet to middle IR portions of the spectrum). The program allows a choice of six reference atmospheres or direct inputs of measured (or assumed) meteorological parameters. Thus, LOWTRAN is an extremely flexible tool which represents a major accomplishment as a general purpose atmospheric transmission code.

LOWTRAN calculates transmission over a selected path by calculating the individual transmittances of separate contributors as though each were acting independently. In order, the elements included in the LOWTRAN calculations are:

- (1) water vapor line absorption from 350 cm^{-1} to $14,500 \text{ cm}^{-1}$
- (2) "uniformly mixed gases" (CO_2 , N_2O , CH_4 , CO , N_2 and O_2) in the intervals 500 to 8060 cm^{-1} and 12970 to 13190 cm^{-1}
- (3) nitrogen continuum between 2080 and 2740 cm^{-1}
- (4) water vapor continuum between 670 and 1400 cm^{-1} and between 2380 and 2850 cm^{-1}
- (5) ozone in the IR between 575 and 3270 cm^{-1} , in the visible between 13000 and 23300 cm^{-1} , and in the UV for wavelengths shorter than 27500 cm^{-1}
- (6) molecular scattering for wavelengths shorter than 2740 cm^{-1}
- (7) nitric acid (HNO_3) in the bands 850 - 920 cm^{-1} , 1275 - 1350 cm^{-1} , and 1675 - 1735 cm^{-1} (LOWTRAN 4 only)
- (8) aerosol scattering and absorption at all wavelengths

LOWTRAN steps down the wavelength scale in 5 cm^{-1} increments and computes individual transmittances $\tau_1(\nu)$, $\tau_2(\nu)$, \dots , $\tau_n(\nu)$ where ν is the frequency in wavenumbers (cm^{-1}). Note that the spectral resolution of the wave band model in LOWTRAN is 20 cm^{-1} so that each $\tau_i(\nu)$ is an average transmittance over 20 wavenumbers. The predictions of LOWTRAN thus approximate the results seen by a low resolution spectrometer (Walsh, 1978:3-24).

After the individual transmittances are computed, the overall average transmission at the wavenumber considered (i.e. the middle of the 20 cm^{-1} interval) is taken as

$$\tau(\nu) = \tau_1(\nu)\tau_2(\nu)\cdots\tau_n(\nu) = \prod \tau_n(\nu) \quad (24)$$

Walsh (1978:3-24) discusses the validity of the assumption implied in Eq 24, ie. that average transmission at ν can be taken as the simple product of the individual contributors at the same wavelength. He concludes that the relation might not be valid where individual average transmittances were low and sharp structure was present within the scale of 20 cm^{-1} for at least two of the contributors. Walsh also cites experimental results which show that the expression holds reasonably well for atmospheric gases in the overall transmission range of about 30-70 per cent.

LOWTRAN Calculation of Individual Transmittances.

LOWTRAN uses some graphical prediction schemes originally suggested by Altshuler (1961) which assign a functional form to the average transmittance over a 20 cm^{-1} interval. The functional forms and their derivations are described in McClatchey et al (1972) and are dependent on the amount of absorber (eg. water content), pressure, temperature and wavelength. The functional forms were put into a kind of nomogram, an example of which is presented in Fig 10. Such charts, for each of the absorber species, were then digitized to form the basis of the LOWTRAN computer program. The aerosol calculations are of major interest in this study and will be considered now in detail.

LOWTRAN Aerosol Treatment. The LOWTRAN program uses two vertical aerosol profiles that describe a "clear" and

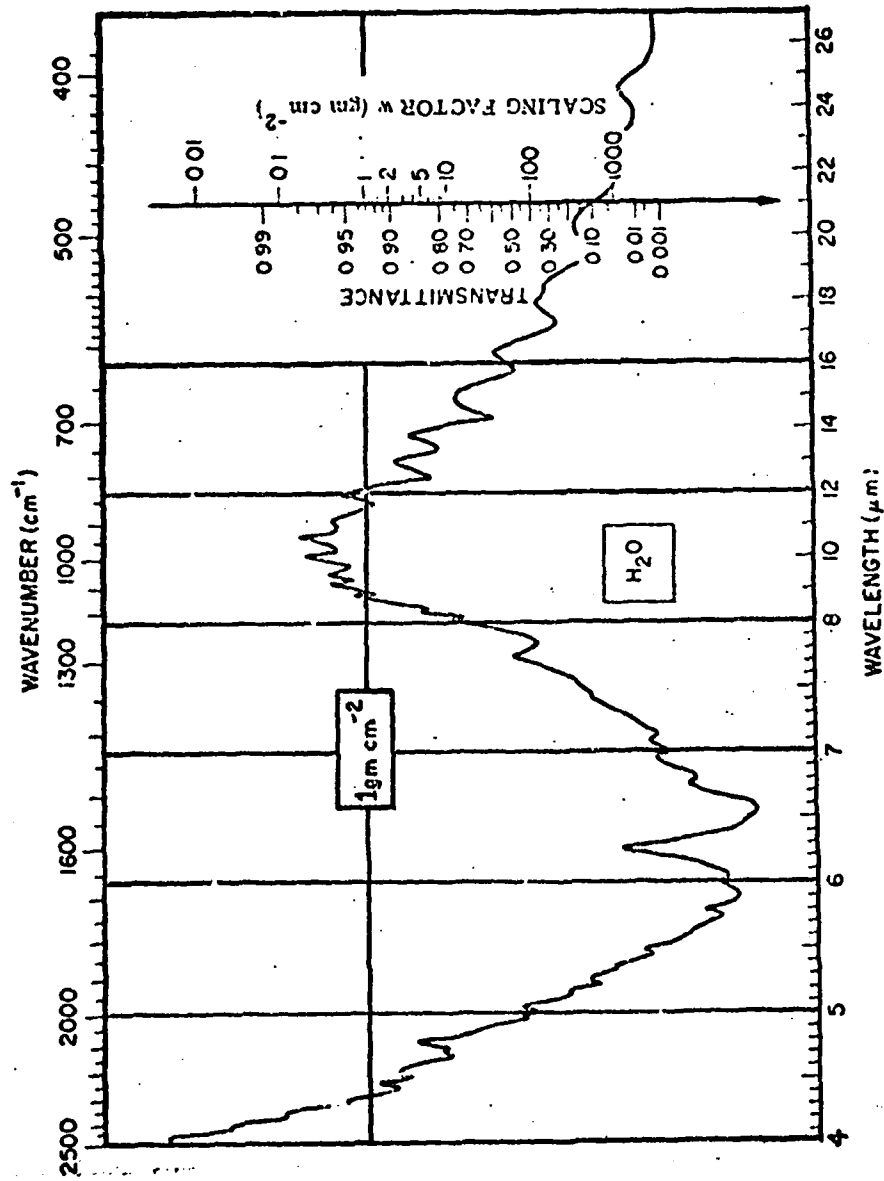


Figure 10. LOWTRAN Prediction Chart for Water Vapor Transmittance (4-26 μm)
 (Ref McClatchey, et al, 1972)

a "hazy" atmosphere corresponding to visibilities (meteorological ranges) of 23 km and 5 km, respectively. The two profiles are based on the following assumptions (Selby and McClatchey, 1975:12ff):

(1) A particle size distribution similar to Deirmendjian's Haze Model C but with the large particle cutoff extended to 100 μm .

(2) The particle size distribution is assumed to remain constant with altitude. Particle densities versus altitude are listed in Table I.

(3) The variation of refractive index with wavelength was obtained from measurements by Volz (1972) who assumed specific mixes of continental (dust-like) and maritime aerosols.

(4) Aerosol extinction coefficients were computed using Mie theory with the assumed particle size distribution and Volz's refractive index values. Extinction coefficients were computed to correspond to several assumed mixes of continental and maritime aerosols. Urban, rural, maritime, tropospheric, and average continental aerosol models are available in LOWTRAN 4, the latest edition of the code. The calculated extinction coefficients are plotted in Figs 11 and 12 for the average continental and maritime aerosol models, respectively.

LOWTRAN Aerosol Interpolation/Extrapolation Scheme.

The relation between the total extinction coefficient β_t and the visibility (or meteorological range) was discussed

Table I

Aerosol Models. Vertical Distributions
 for a "Clear" and "Hazy" Atmosphere
 (Ref McClatchey, 1972)

Altitude (km)	PARTICLE DENSITY N (PARTICLES PER cm ³)	
	23 km Visibility Clear	5 km Visibility Hazy
0	2.828E+03	1.378E+04
1	1.244E+03	5.030E+03
2	5.371E+02	1.844E+03
3	2.256E+02	6.731E+02
4	1.192E+02	2.453E+02
5	8.987E+01	8.987E+01
6	6.337E+01	6.337E+01
7	5.890E+01	5.890E+01
8	6.069E+01	6.069E+01
9	5.818E+01	5.818E+01
10	5.675E+01	5.675E+01
11	5.317E+01	5.317E+01
12	5.585E+01	5.585E+01
13	5.156E+01	5.156E+01
14	5.048E+01	5.048E+01
15	4.744E+01	4.744E+01
16	4.511E+01	4.511E+01
17	4.458E+01	4.458E+01
18	4.314E+01	4.314E+01
19	3.634E+01	3.634E+01
20	2.667E+01	2.667E+01
21	1.933E+01	1.933E+01
22	1.455E+01	1.455E+01
23	1.113E+01	1.113E+01
24	8.826E+00	8.826E+00
25	7.429E+00	7.429E+00
30	2.238E+00	2.238E+00
35	5.890E-01	5.890E-01
40	1.550E-01	1.550E-01
45	4.082E-02	4.082E-02
50	1.078E-02	1.078E-02
70	5.550E-05	5.550E-05
100	1.969E-08	1.969E-08

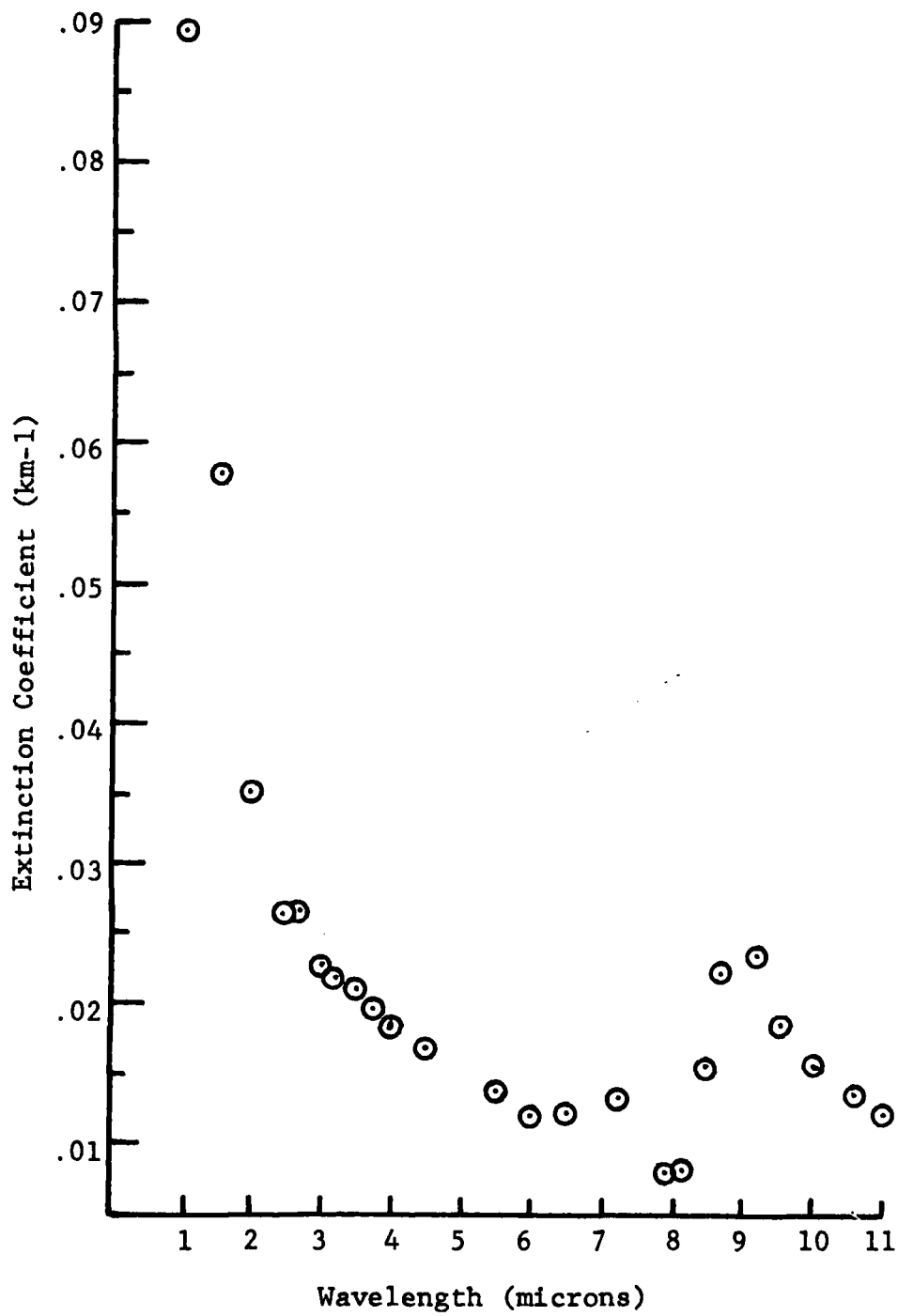


Figure 11. LOWTRAN Average Continental Aerosol Extinction Coefficients (Sea Level Values)

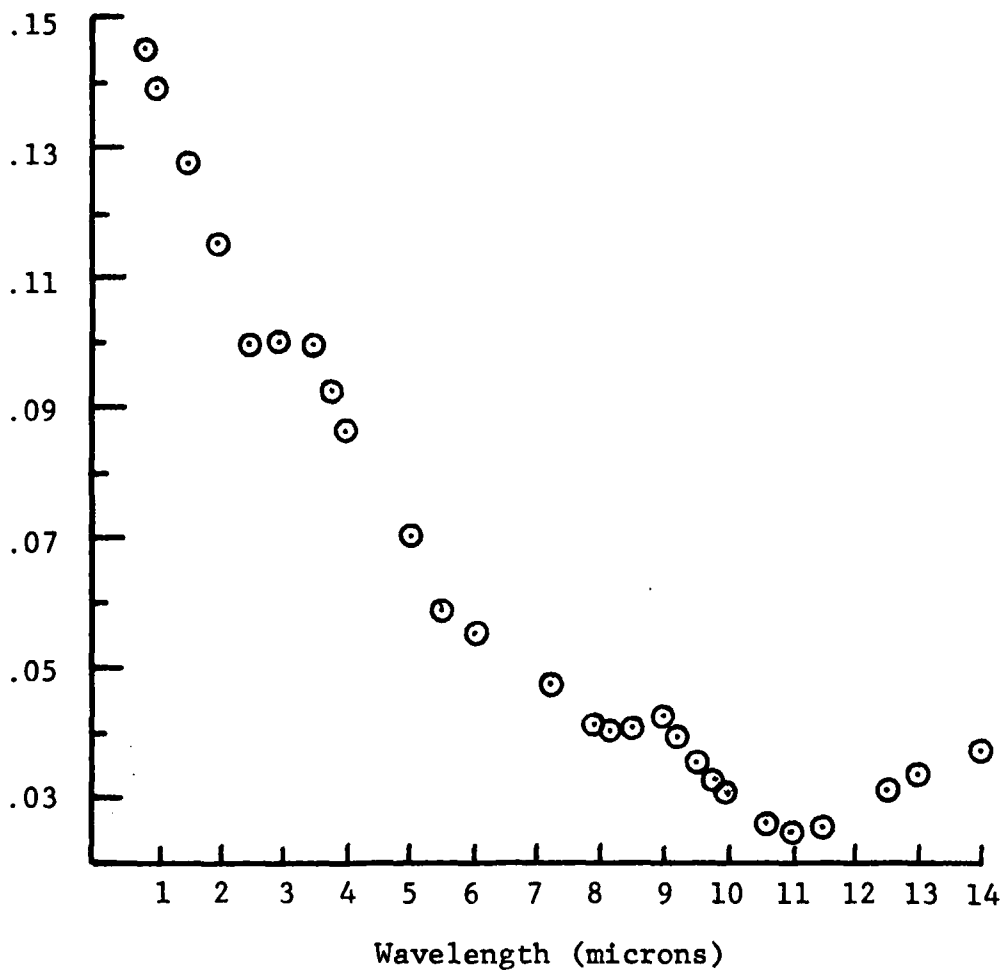


Figure 12. LOWTRAN Maritime Aerosol Extinction Coefficients (Sea Level Values)

earlier. Middleton (1952) reported the Koschmeider relationship which holds well at a wavelength of 0.55 μm , the wavelength at which the human eye has its greatest sensitivity. Equation 27 defines the total extinction coefficient β_t in terms of visibility as

$$\beta_t = \frac{1}{\text{VIS}} \ln \frac{1}{T} = \frac{3.91}{\text{VIS}} \quad (27)$$

where

VIS = the horizontal visibility or meteorological range (km)

T = the threshold value of brightness contrast for the eye (T=0.02 for daylight and large black objects against the sky)

Eq 27 provides the link between the concepts of "clear" (23 km visibility) and "hazy" (5 km visibility) aerosol models as used in LOWTRAN. The following development will make this link more apparent.

From Eq 27 the total extinction coefficient may be written as the sum of an aerosol extinction coefficient β_a and a molecular extinction coefficient β_m . Thus,

$$\beta_t = \beta_a + \beta_m = \frac{3.91}{\text{VIS}} \quad (28)$$

and

$$\beta_a = \frac{3.91}{\text{VIS}} - \beta_m \quad (29)$$

From Mie theory calculations the aerosol extinction coefficient is seen to be directly proportional to the aerosol

number density $N(z)$. We can then write

$$N(z) = \frac{a(z)}{\text{VIS}} + b(z) \quad (30)$$

where $a(z)$ and $b(z)$ are constants at any altitude z . In Eq 30, $b(z)$ is proportional to the molecular scattering coefficient at $0.55 \mu\text{m}$ and molecular absorption at $0.55 \mu\text{m}$ has been assumed negligible. The coefficients $a(z)$ and $b(z)$ are determined by linear interpolation between the values of $N(z)$ for 5 km and 23 km visibilities.

The limitation of the LOWTRAN method discussed above is the assumed prototypical aerosol distributions, indices of refraction, and aerosol extinction coefficients derived using those assumed parameters. No realistic alternative to this semi-empirical approach has yet been conclusively demonstrated. However, recent measurements at Grafenwohr, FRG, (Roberts, 1978) show that for a particular aerosol and spectral region the extinction is most critically dependent upon the volume of particulate in the atmospheric path and not so much upon the detailed description of the distribution function. Roberts recommended that LOWTRAN's maritime aerosol model be used in all low visibility situations - a suggestion incorporated in subroutine HAZE written for ASDIR.

III. Results and Discussion

The approach taken to incorporate the LOWTRAN aerosol treatment into ASDIR was one which involved several compromises. The ASDIR program is a large and long-running program so that one of the first requirements was to keep the added aerosol subroutines as short as possible without substantially sacrificing accuracy. Thus it was decided to curve fit several LOWTRAN aerosol parameters to obtain simple analytical expressions which reduced both the core-storage requirements and running time of the aerosol calculations. Curve fits were obtained for (1) particle densities as a function of altitude, (2) the extinction coefficients for the average continental and maritime aerosol models, and (3) for actual LOWTRAN calculated values of an important parameter - the equivalent sea level path for vertical atmospheric paths.

Particle Densities

The assumed aerosol vertical distributions for LOWTRAN given in Table I are used in the calculations of equivalent path through the aerosol environment. The table values for the 23 km visibility ("clear") case and the 5 km ("hazy") case are plotted in Fig 13. Note that at altitudes above the 5 km mixing layer the assumed particle densities are equal for all visibility ranges. The values were curve fit using straight line segments (on semi-log paper) to obtain

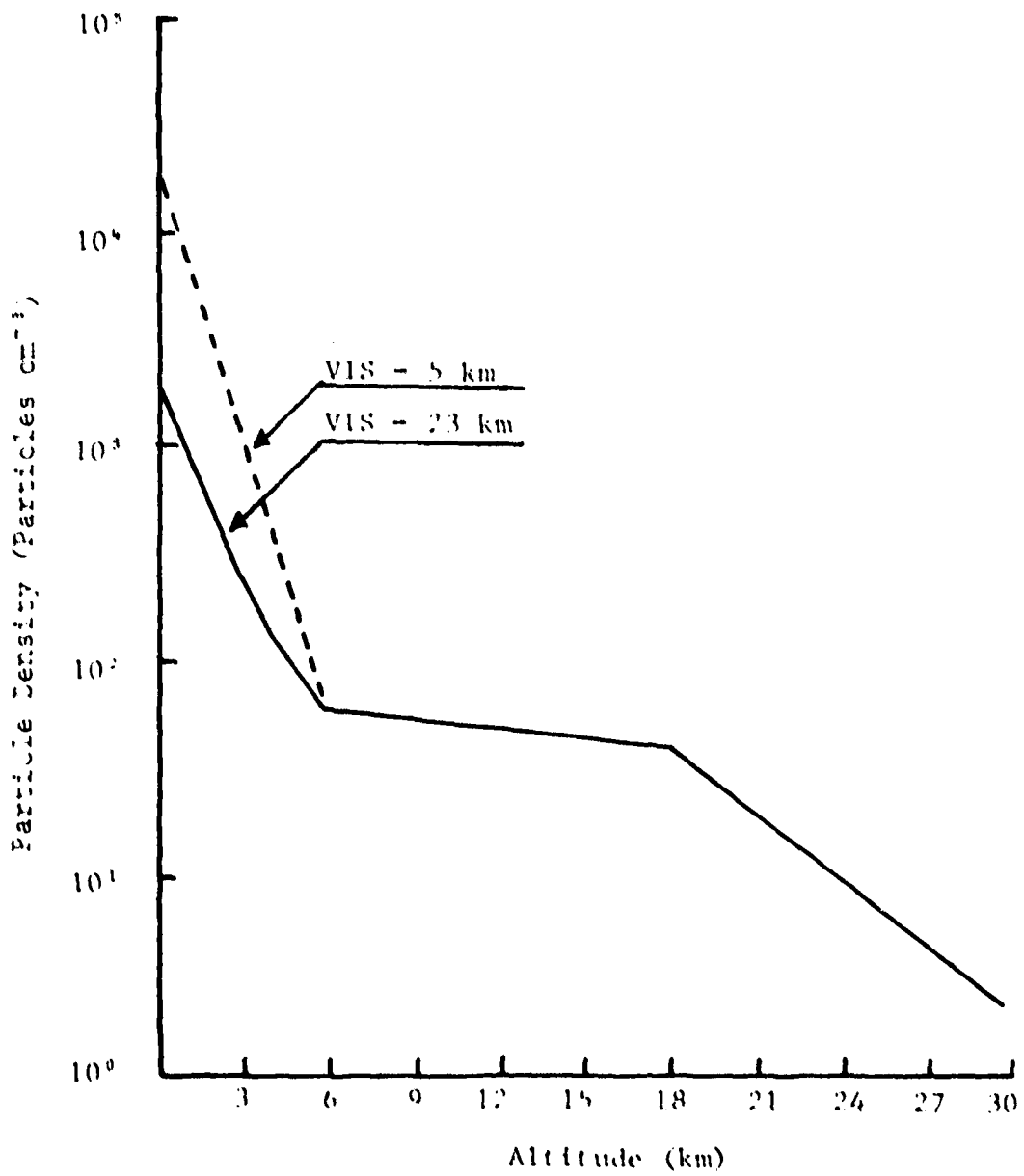


Figure 13. Assumed Aerosol Vertical Distributions

Table II
Derived Expressions for Particle Density

z (km)	$N_{23}(z)$ - "clear"	$N_5(z)$ - "hazy"
$0 < z \leq 3$	$2828 \times 10^{-.36z}$	$13870 \times 10^{-.437z}$
$3 < z \leq 4$	$1529 \times 10^{-.277z}$	"
$4 < z \leq 5$	$422 \times 10^{-.137z}$	"
$5 < z \leq 6$	$422 \times 10^{-.137z}$	Same as $N_{23}(z)$
$6 < z \leq 18$	$77 \times 10^{-.0139z}$	Same as $N_{23}(z)$
$18 < z \leq 30$	$3651 \times 10^{-.107z}$	Same as $N_{23}(z)$
$30 < z$	Assumed zero	Same as $N_{23}(z)$

the functions listed in Table II. The expressions for $N_{23}(z)$ and $N_5(z)$ are used to interpolate for the total particle density $N(z)$ using Eq 30 in which the values $a(z)$ and $b(z)$ depend on $N_{23}(z)$ and $N_5(z)$ at a given altitude as follows:

$$a(z) = (N_5(z) - N_{23}(z)) / (1/5 - 1/23) \quad (31-a)$$

$$b(z) = (N_{23}(z)/5 - N_5(z)/23) / (1/5 - 1/23) \quad (31-b)$$

These expressions were used in HAZE only for computing the equivalent sea level path length for horizontal transmission paths given by

$$\bar{R} = R(N(z)/N_0) \quad (32)$$

where R is actual slant range as before. For the general case of slant paths, a different approach was followed and is described in a later section.

Extinction Coefficients

Piecemeal curve fits were obtained for the average continental and maritime extinction coefficients plotted in Figs 11 and 12, respectively. The curve fits were partially obtained using the IMSL packages available on the CDC 6600 computer at Wright-Patterson AFB, OH. The resulting analytical expressions are given as Tables III and IV for the two selected aerosol models. Maximum errors between the given LOWTRAN values and corresponding values computed using the curve fit expressions were 6 per cent for the average continental model and about 5 per cent for the maritime model. The small errors that are seen in the computer-generated transmission plots for LOWTRAN and subroutine HAZE are largely due to these slight discrepancies in calculated extinction coefficients. However, the benefits of the curve fits were a reduction in core storage requirements and logic simplification - both desirable features for inclusion into ASDIR.

Equivalent Sea Level Path Lengths

For transmission along a slant path LOWTRAN first computes an equivalent sea level vertical path length (AV) for the altitudes Z_1 and Z_2 at each end of the actual path. This vertical equivalent path is a measure of the aerosol

Table III

Curve Fit Expressions for LOWTRAN Average Continental
Aerosol Extinction Coefficients (Sea Level Values)

(Note: Values are rounded to three significant figures.)

Wavelength - λ (μm)	Extinction Coefficient (km^{-1})
$0.86 \leq \lambda \leq 2.0$	$-0.064\lambda + 0.163$
$2.0 < \lambda < 7.2$	$0.001\lambda^2 - 0.015\lambda + 0.058$
$7.2 \leq \lambda < 7.9$	$-0.008\lambda + 0.069$
$7.9 \leq \lambda \leq 8.2$	$0.001\lambda + 0.001$
$8.2 < \lambda \leq 9.0$	$-0.001\lambda^2 + 0.171\lambda - 0.802$
$9.0 < \lambda \leq 9.2$	0.024
$9.2 < \lambda \leq 14.0$	$0.011 - (1.5 \times 10^{-4})\lambda + 139 \exp(-\lambda)$
$14.0 < \lambda$	0.010

Table IV

Curve Fit Expressions for LOWTRAN Maritime Aerosol
Extinction Coefficients (Sea Level Values)

(Note: Values are rounded to three significant figures.)

Wavelength - λ (μm)	Extinction Coefficient (km^{-1})
$0.86 \leq \lambda \leq 2.5$	$-0.027\lambda + 0.167$
$2.5 < \lambda \leq 3.5$	0.100
$3.5 < \lambda \leq 8.2$	$0.002\lambda^2 - 0.038\lambda + 0.204$
$8.2 < \lambda < 9.0$	$-0.010\lambda^2 - 0.177\lambda - 0.734$
$9.0 \leq \lambda < 11.0$	$0.003\lambda^2 - 0.061\lambda + 0.380$
$11.0 \leq \lambda \leq 14.0$	$0.004\lambda - 0.020$
$14.0 < \lambda$	0.039

amounts in the atmosphere above the altitude z and is given by the equation

$$AV = \int_z^{\infty} \frac{N(z)}{N_0} dz \quad (33)$$

The quantity AV is a function of both visibility and altitude through the dependence of $N(z)$ on those two variables. To accurately reproduce the LOWTRAN values for AV in the HAZE subroutine LOWTRAN runs were made to obtain actual values for the somewhat lengthy integrations required by Eq 33. The AV values were plotted (see Appendix A) and curve fits were obtained as functions of VIS (visibility) and z (altitude in km). The results of the curve fits are also given in Appendix A.

According to the LOWTRAN documentation (McClatchey et al, 1972:35) the overall equivalent path length for a slant path is given by Eq 34.

$$\bar{R} = (AV(z_1) - AV(z_2))R/(z_2 - z_1) \quad (34)$$

However, LOWTRAN calculations for \bar{R} did not match exactly with the expected results using Eq 34. That is, using LOWTRAN's own calculated values of $AV(z_1)$ and $AV(z_2)$ for a given range R and altitudes z_1 and z_2 , LOWTRAN's value of \bar{R} differed as much as 9 per cent from that determined by Eq 34. The error was found to be dependent upon VIS.

A formula was devised to calculate this variance and, in effect, a correction factor (CFAC) was programmed into the HAZE subroutine to accurately reproduce the LOWTRAN values for \bar{R} . The listing of subroutine HAZE is given in Appendix C.

Aerosol Transmission Calculations

To determine the accuracy of the HAZE subroutine in duplicating LOWTRAN's aerosol transmission calculations 16 selected cases were run using two aerosol models and varying visibilities and path lengths. Visibilities were chosen 2, 5, 10, and 23 km representing a variance from very "hazy" to "clear" atmospheres. Ranges of 4 and 10 km were selected as representative of short to medium range IR missile detector operating ranges. Figures 14-29 give the plotted results of aerosol transmission (other attenuators not included) and show the excellent agreement obtained between the HAZE and LOWTRAN results. No detailed statistical analysis of the small errors is deemed appropriate because of the empirical nature of the LOWTRAN methodology. The major value of LOWTRAN and HAZE aerosol predictions lies in showing in what regimes aerosol effects are significant rather than in absolute values of transmission. It is clear from the results, however, that for even relatively "clear" atmospheres, excluding aerosol effects (as ASDIR has done) can introduce errors in overall transmission calculations of 20 per cent or more dependent upon the aerosol model selected.

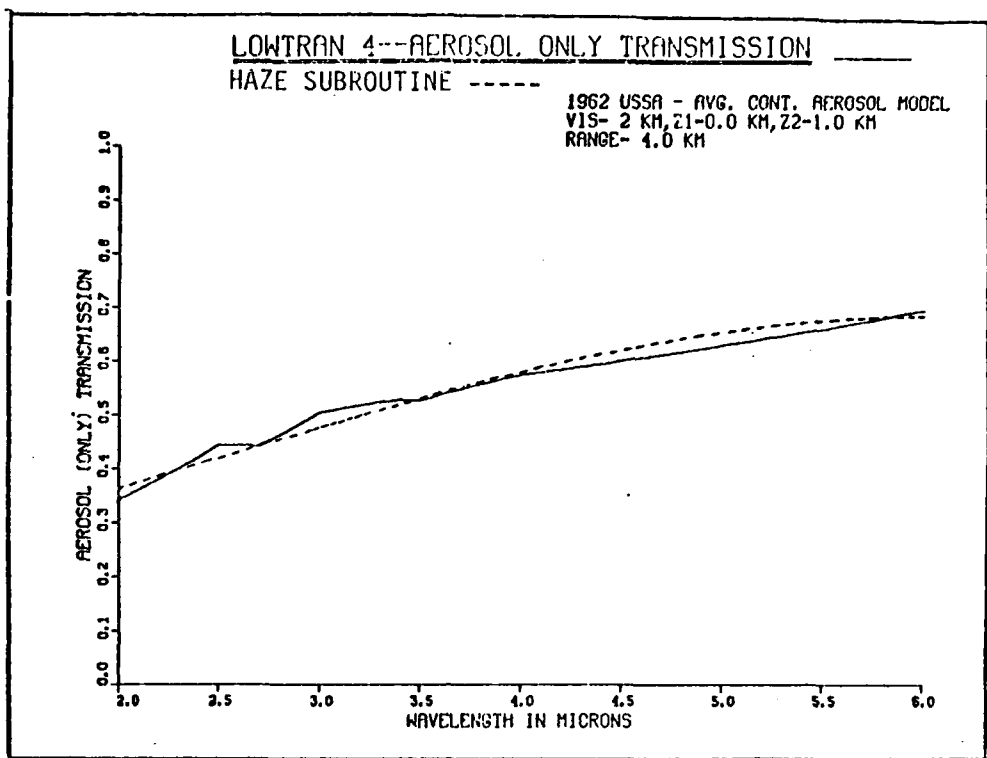


Figure 14. LOWTRAN/HAZE Subroutine Comparison (2-6 μm)

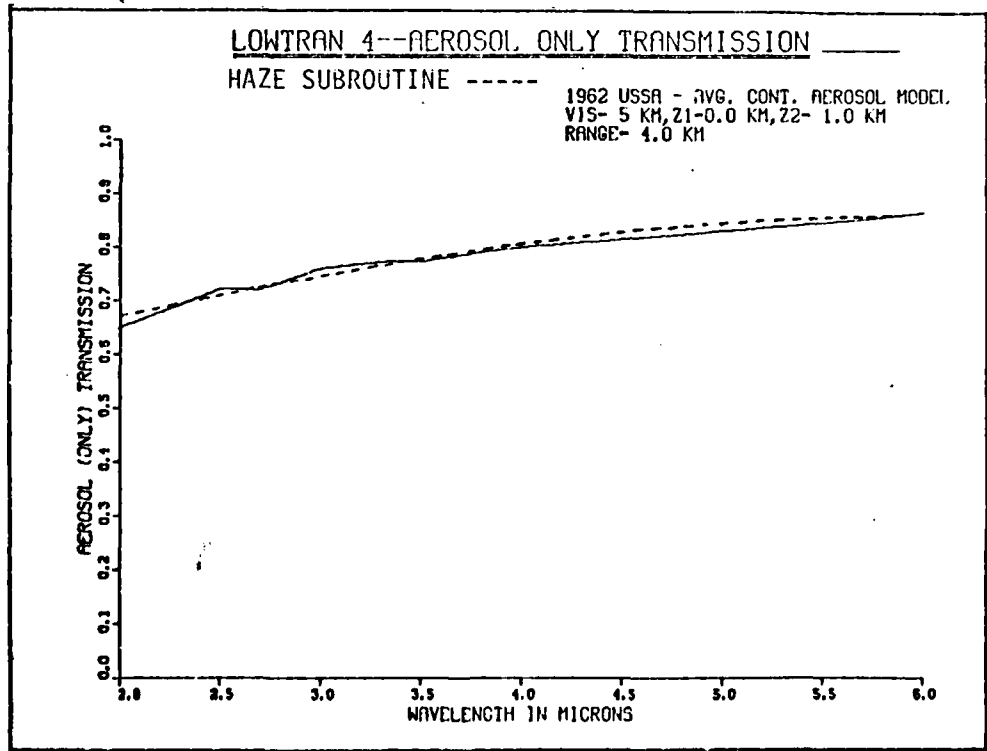


Figure 15. LOWTRAN/HAZE Subroutine Comparison (2-6 μm)

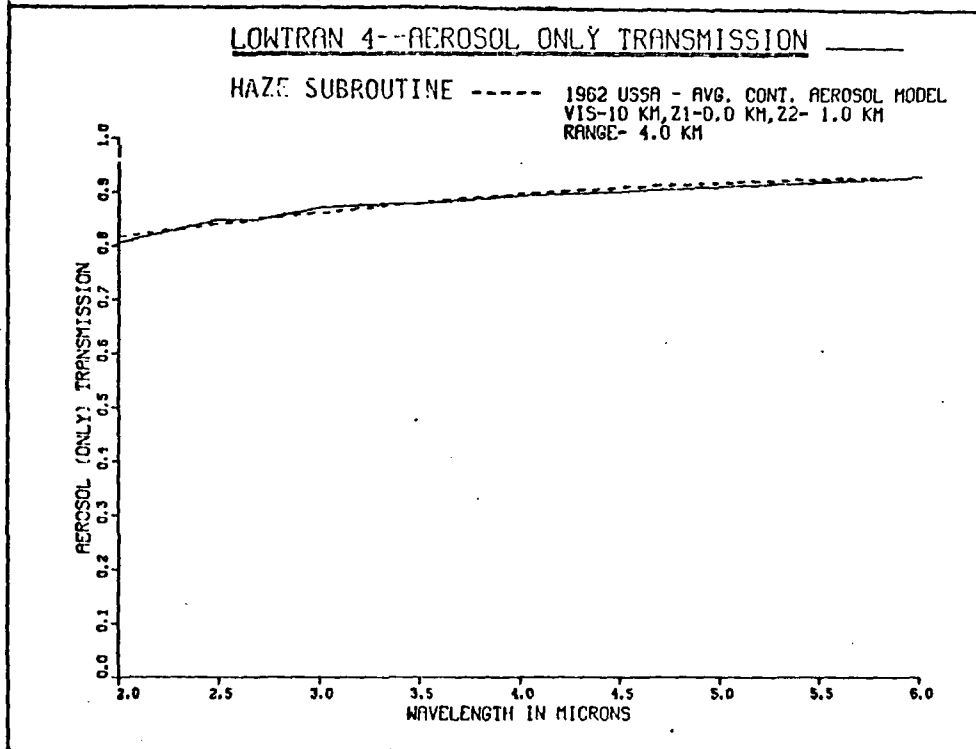


Figure 16. LOWTRAN/HAZE Subroutine Comparison (2-6 μm)

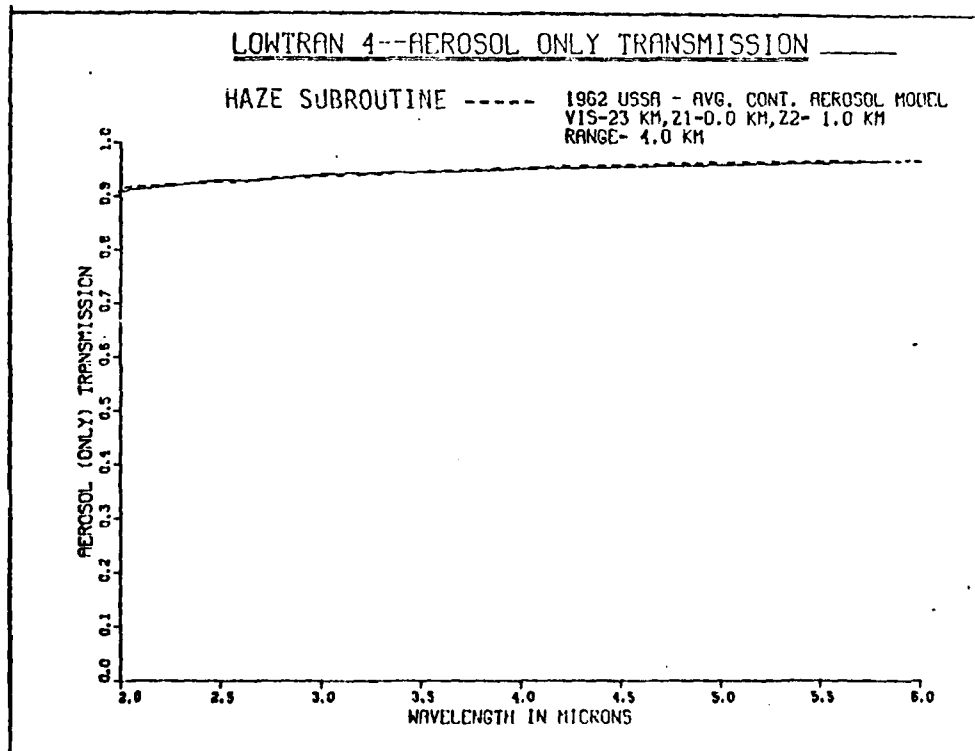


Figure 17. LOWTRAN/HAZE Subroutine Comparison (2-6 μm)

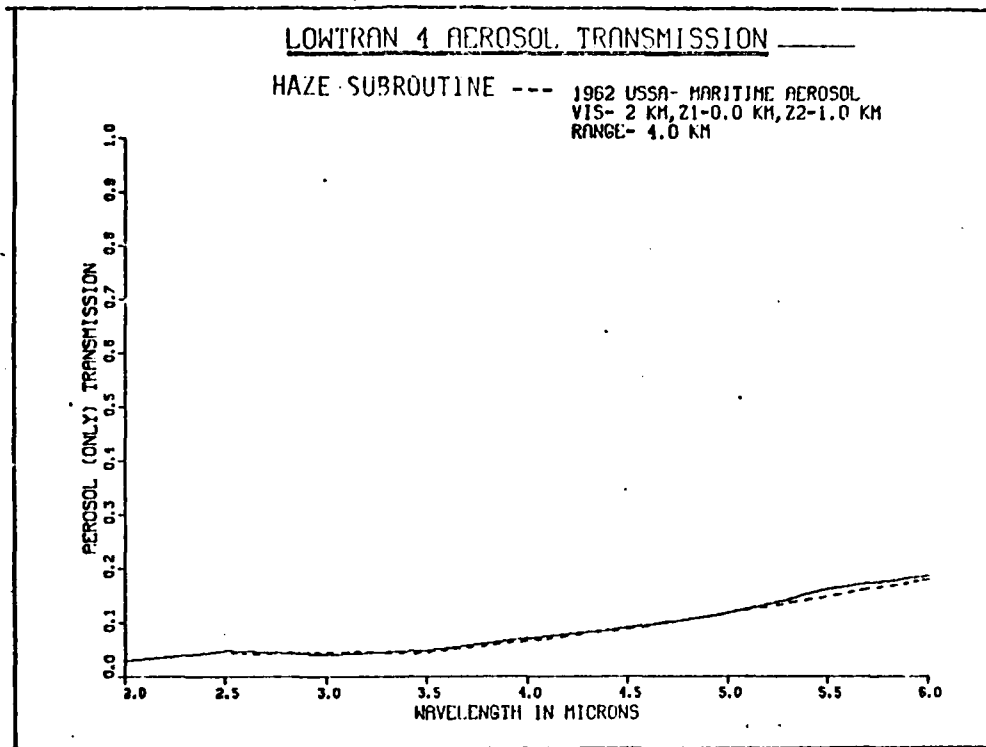


Figure 18. LOWTRAN/HAZE Subroutine Comparison (2-6 μm)

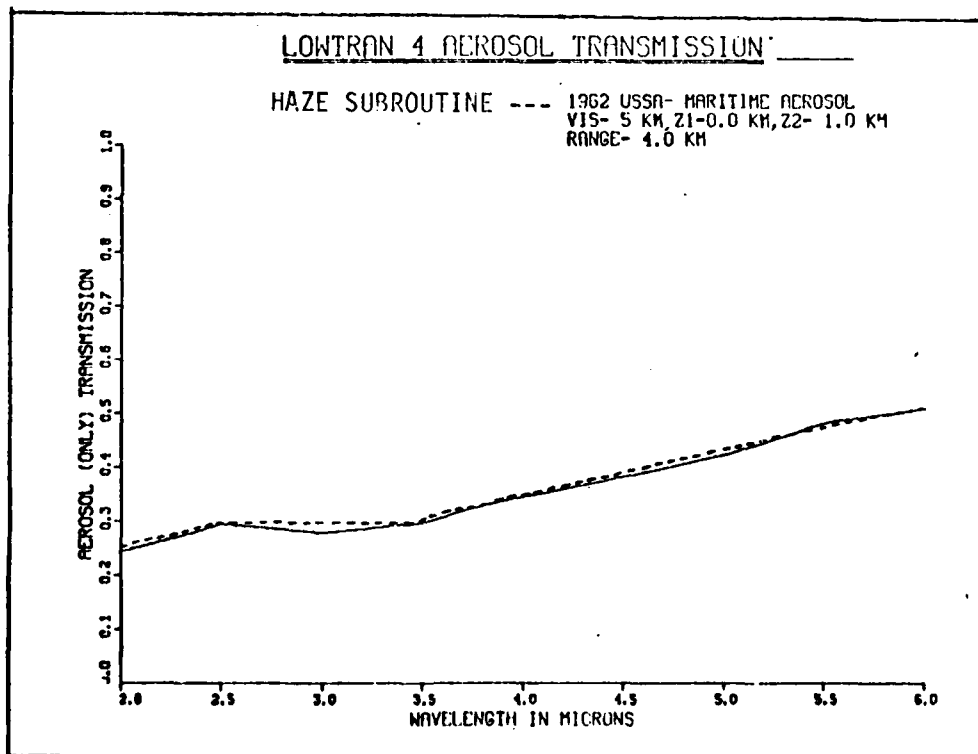


Figure 19. LOWTRAN/HAZE Subroutine Comparison (2-6 μm)

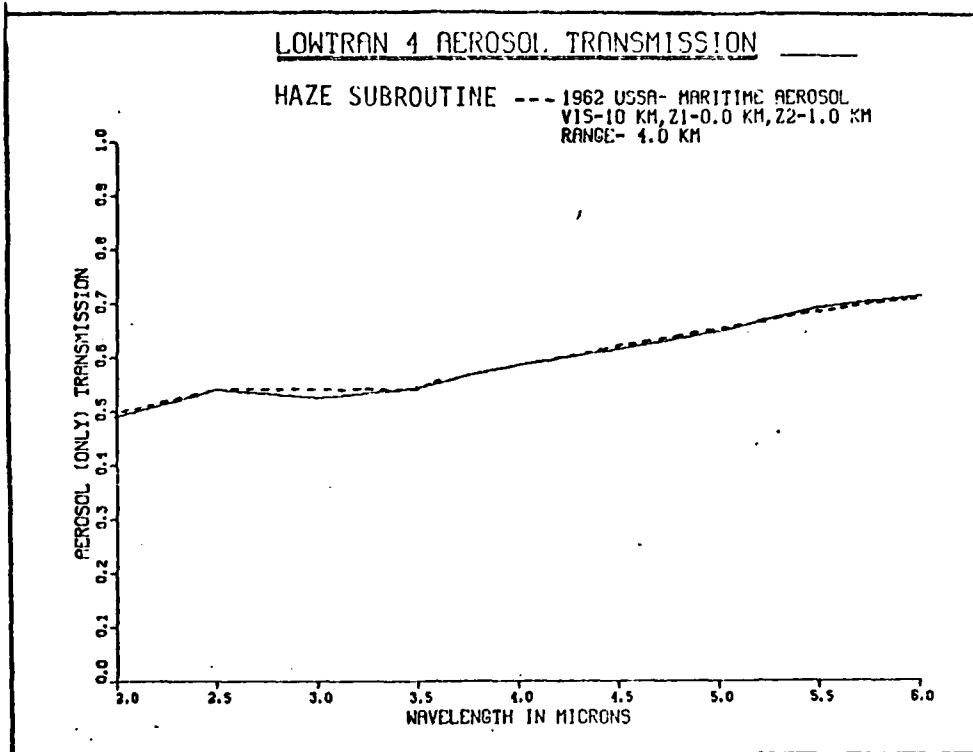


Figure 20. LOWTRAN/HAZE Subroutine Comparison (2-6 μm)

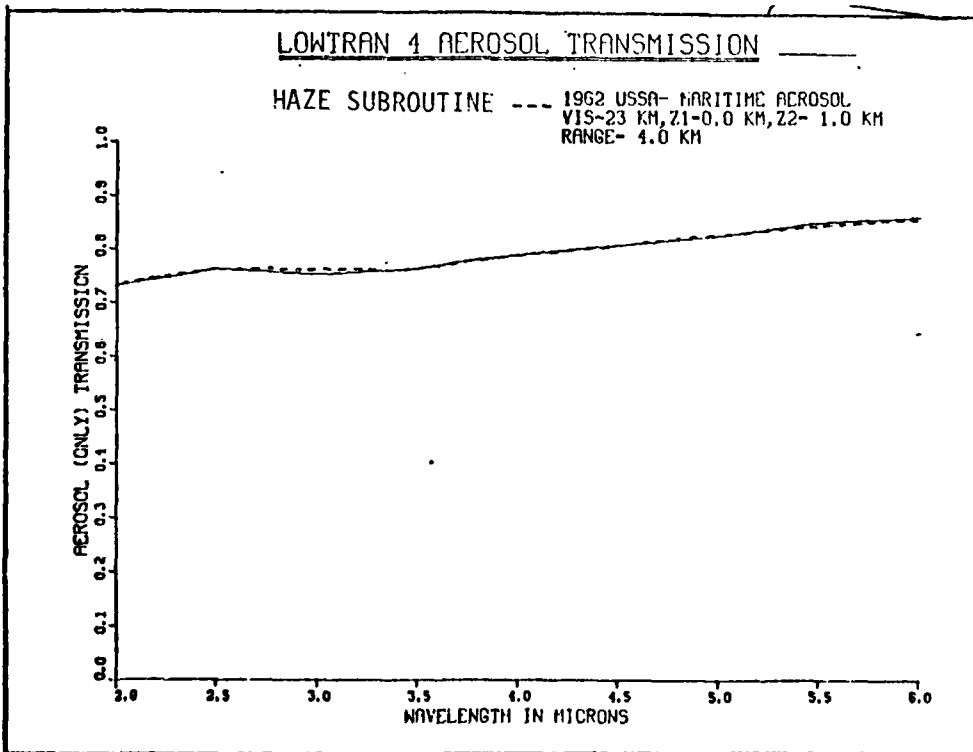


Figure 21. LOWTRAN/HAZE Subroutine Comparison (2-6 μm)

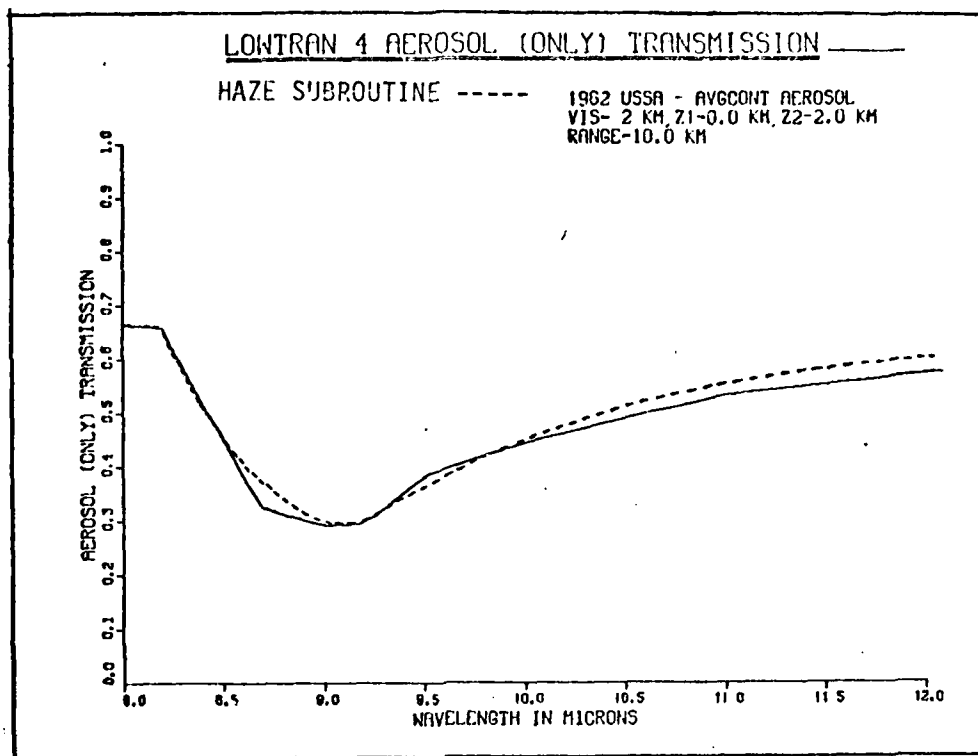


Figure 22. LOWTRAN/HAZE Subroutine Comparison (8-12 μm)

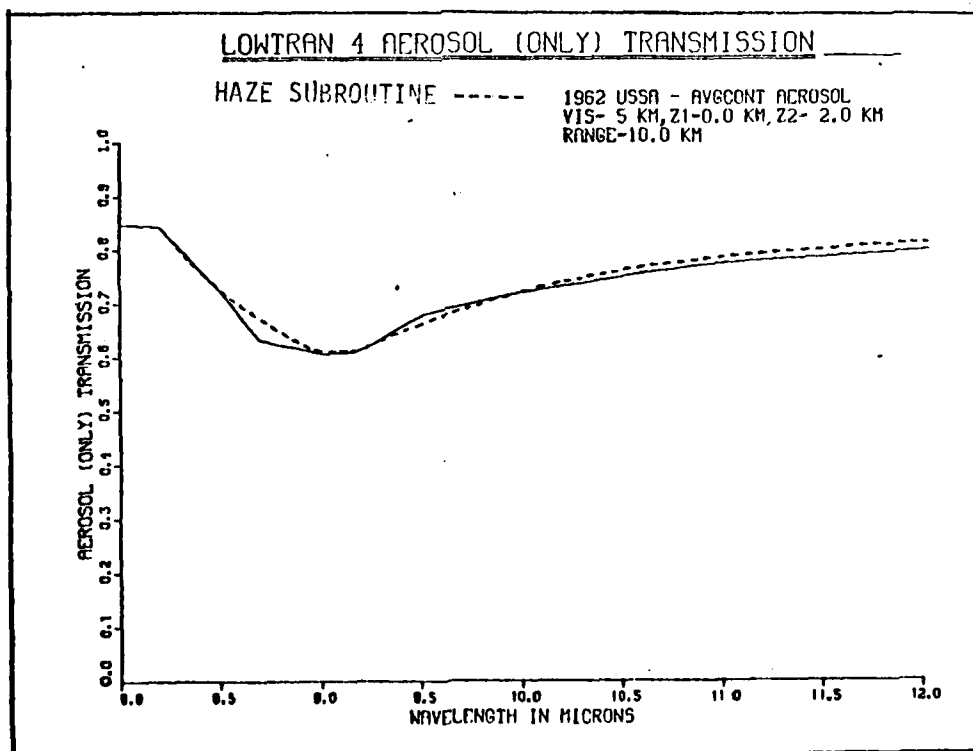


Figure 23. LOWTRAN/HAZE Subroutine Comparison (8-12 μm)

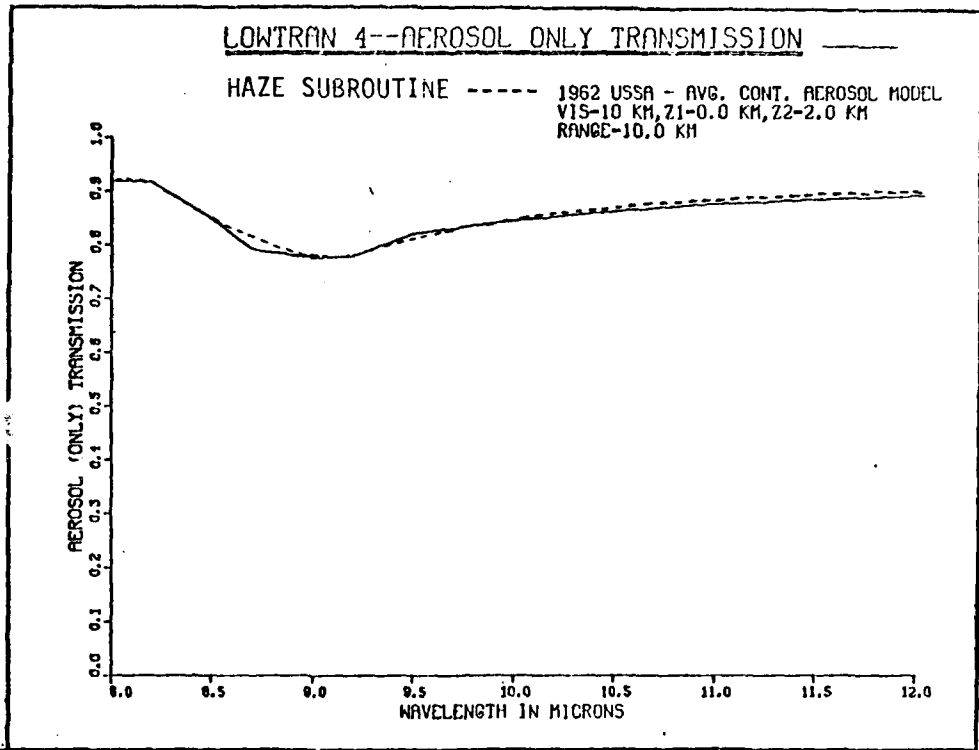


Figure 24. LOWTRAN/HAZE Subroutine Comparison (8-12 μ m)

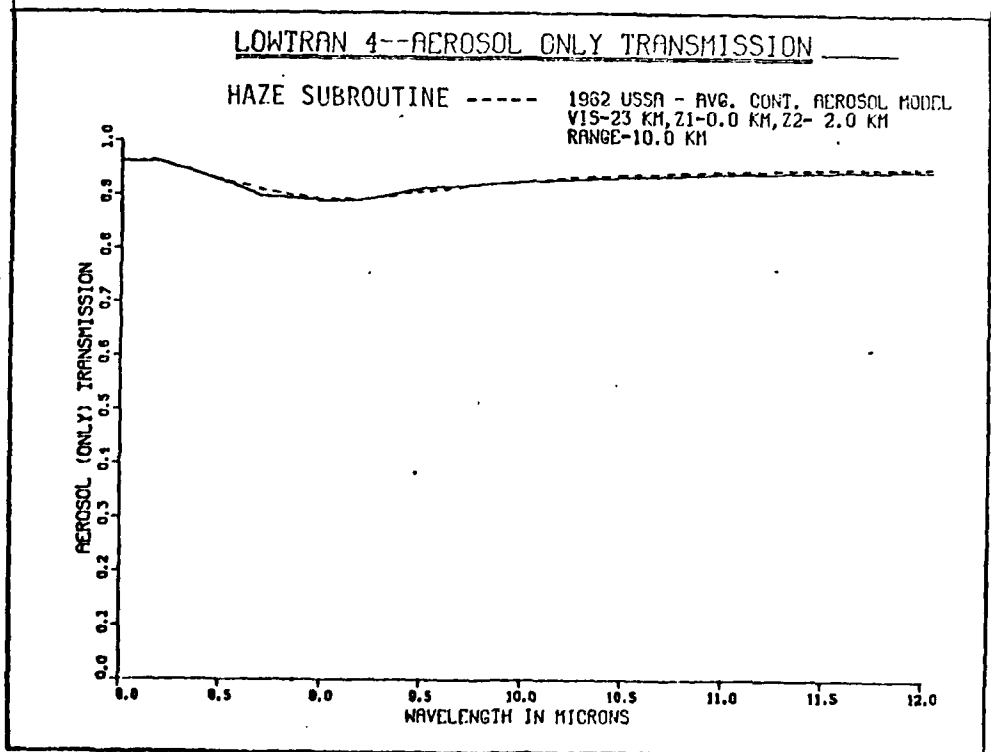


Figure 25. LOWTRAN/HAZE Subroutine Comparison (8-12 μ m)

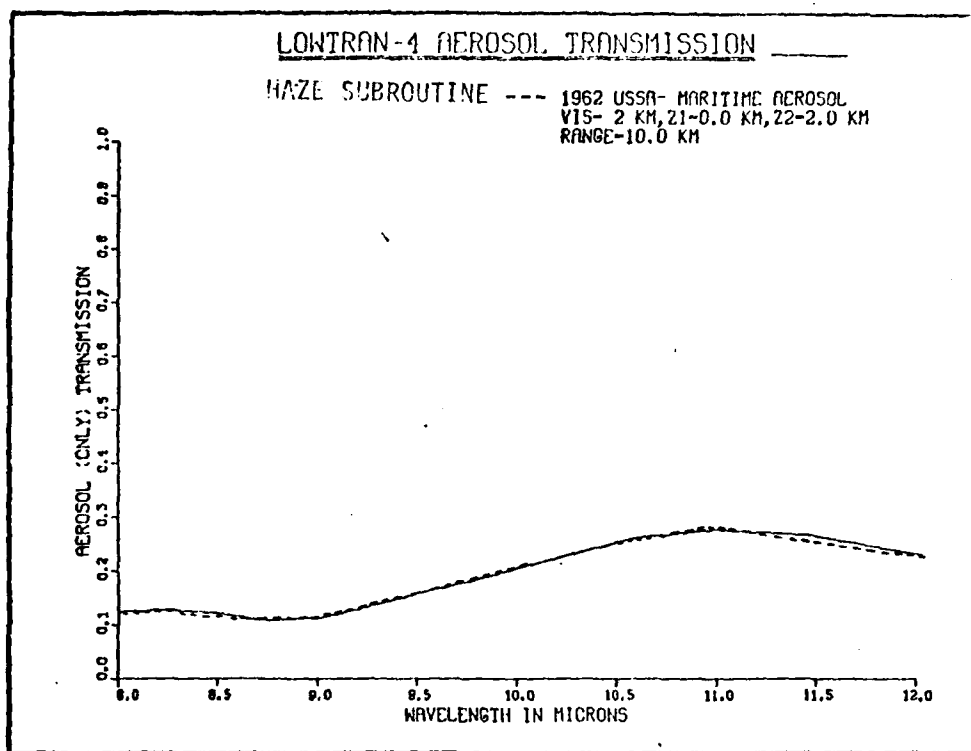


Figure 26. LOWTRAN/HAZE Subroutine Comparison (8-12 μm)

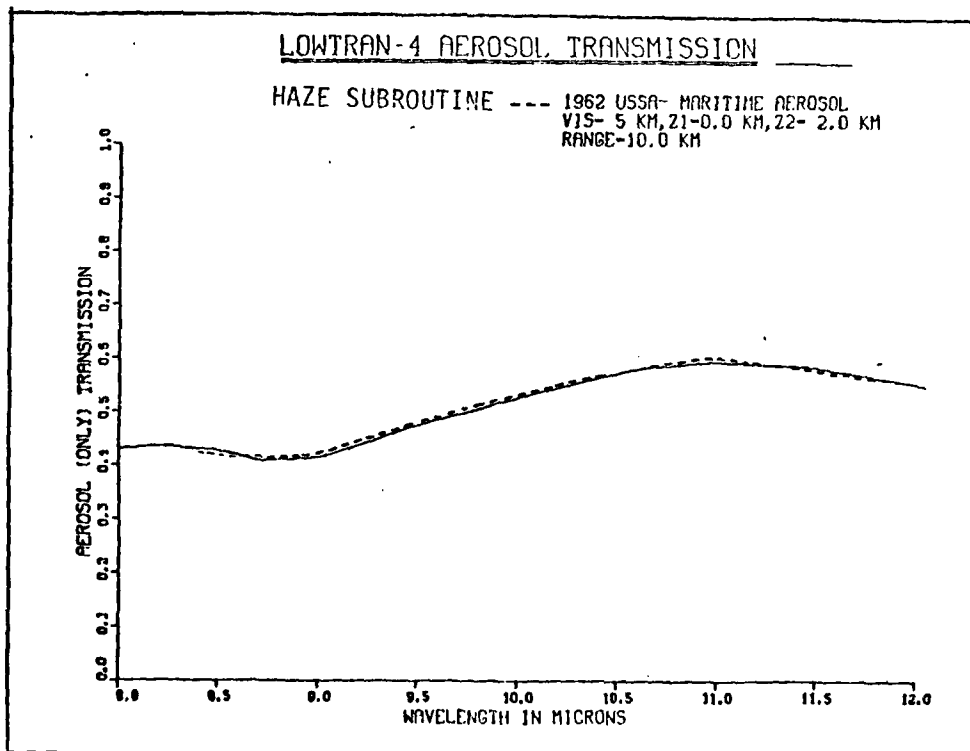


Figure 27. LOWTRAN/HAZE Subroutine Comparison (8-12 μm)

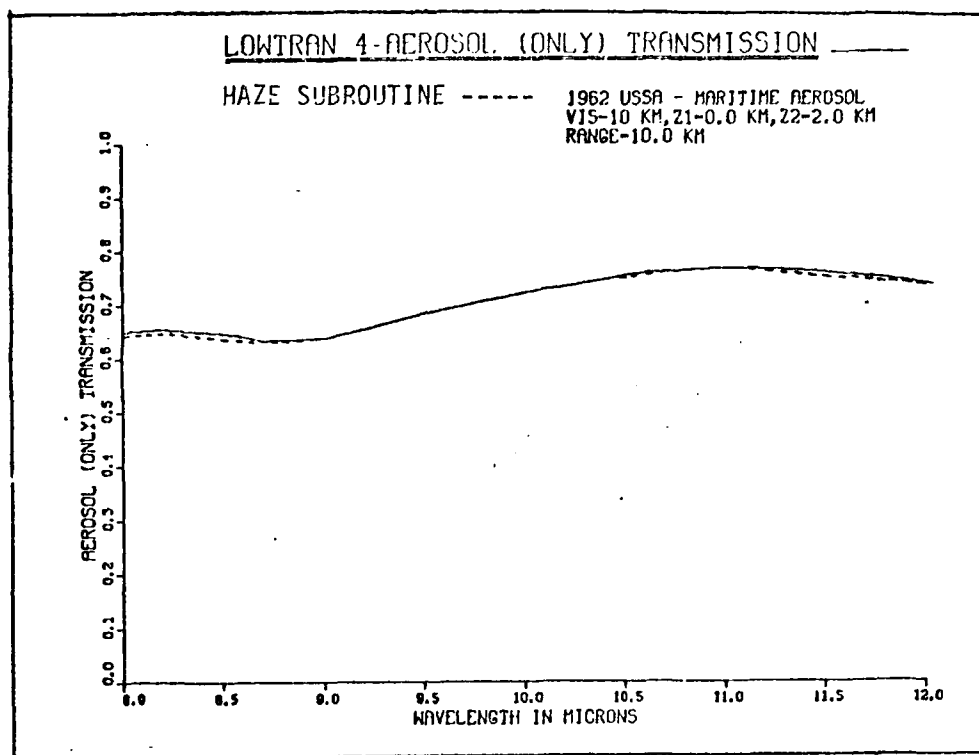


Figure 28. LOWTRAN/HAZE Subroutine Comparison (8-12 μm)

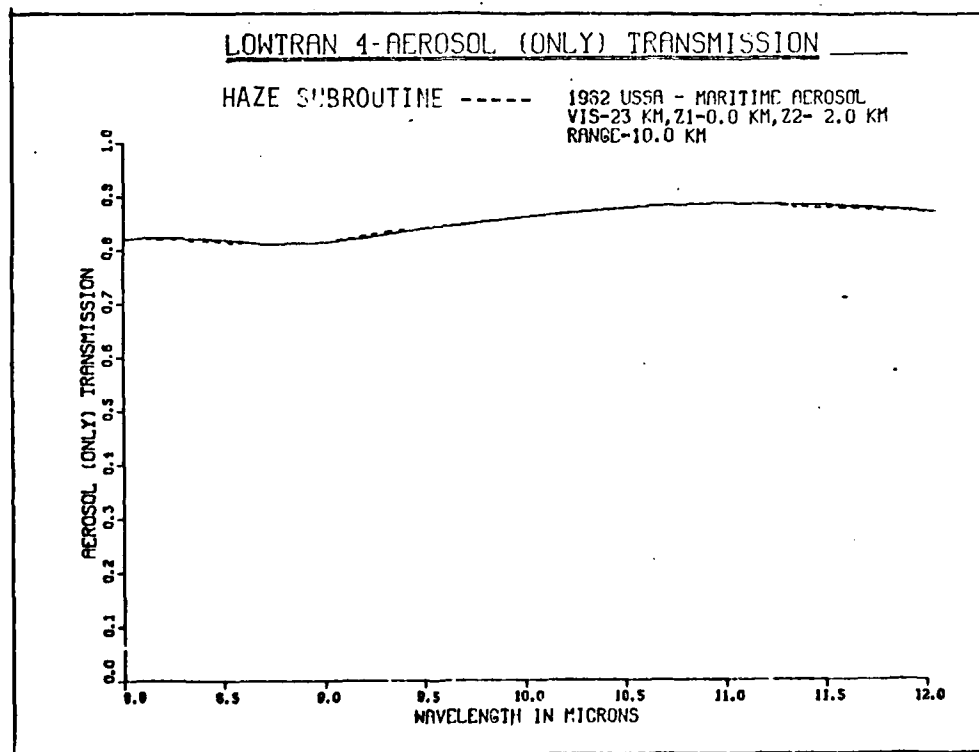


Figure 29. LOWTRAN/HAZE Subroutine Comparison (8-12 μm)

Comparison of the Unmodified ASDIR and LOWTRAN. To get a baseline comparison between the unmodified ASDIR program and LOWTRAN (without aerosols) several cases were run with the resulting plots placed on the same graphs. Figures 30-32 display these comparisons for two low altitude cases and one high altitude situation. The "target" in ASDIR was modeled as a small black body emitter at 500 R.

It is apparent from the figures that ASDIR (solid line in these plots) does not show the same small variations in transmission as does LOWTRAN. This is because LOWTRAN includes several absorbers (eg. O_3 , N_2O , CH_4 , N_2 , and O_3) that ASDIR does not include. ASDIR was written as a time-wise tool for preliminary IR engineering design and thus neglected those minor atmospheric constituents.

The major disagreement between ASDIR and LOWTRAN lies in the region between 4.5 and about 4.8 μm . In this region, absorption by nitrogen continuum is significant. LOWTRAN computes a smaller N_2 continuum absorption in that region than does ASDIR. Resolution of these differences is beyond the scope of this independent study, and these results are presented only for a comparative assessment of the two programs.

Addition of the HAZE Subroutine into ASDIR

The accuracy of the HAZE subroutine in duplicating LOWTRAN's aerosol transmission calculations has been demonstrated. The HAZE subroutine was installed into ASDIR and

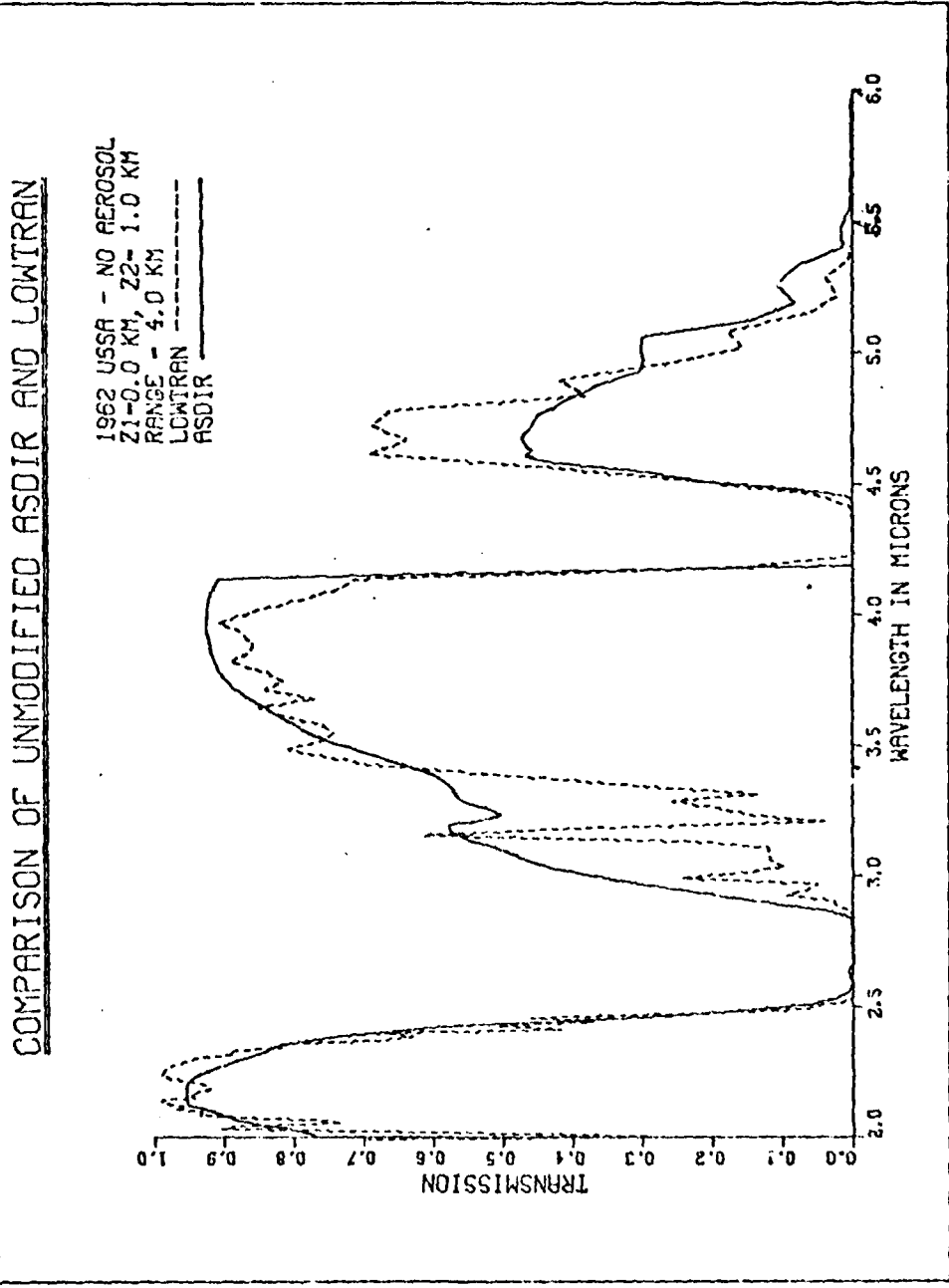


Figure 30. Low Altitude Comparison (Case 1) Between the Unmodified ASDIR and LOWTRAN Program Results

COMPARISON OF UNMODIFIED ASDIR AND LOWTRAN

1962 USSA - NO AEROSOL
Z1-0.0 KM, Z2- 2.0 KM
RANGE- 10.0 KM
LOWTRAN - - - - -
ASDIR - - - - -

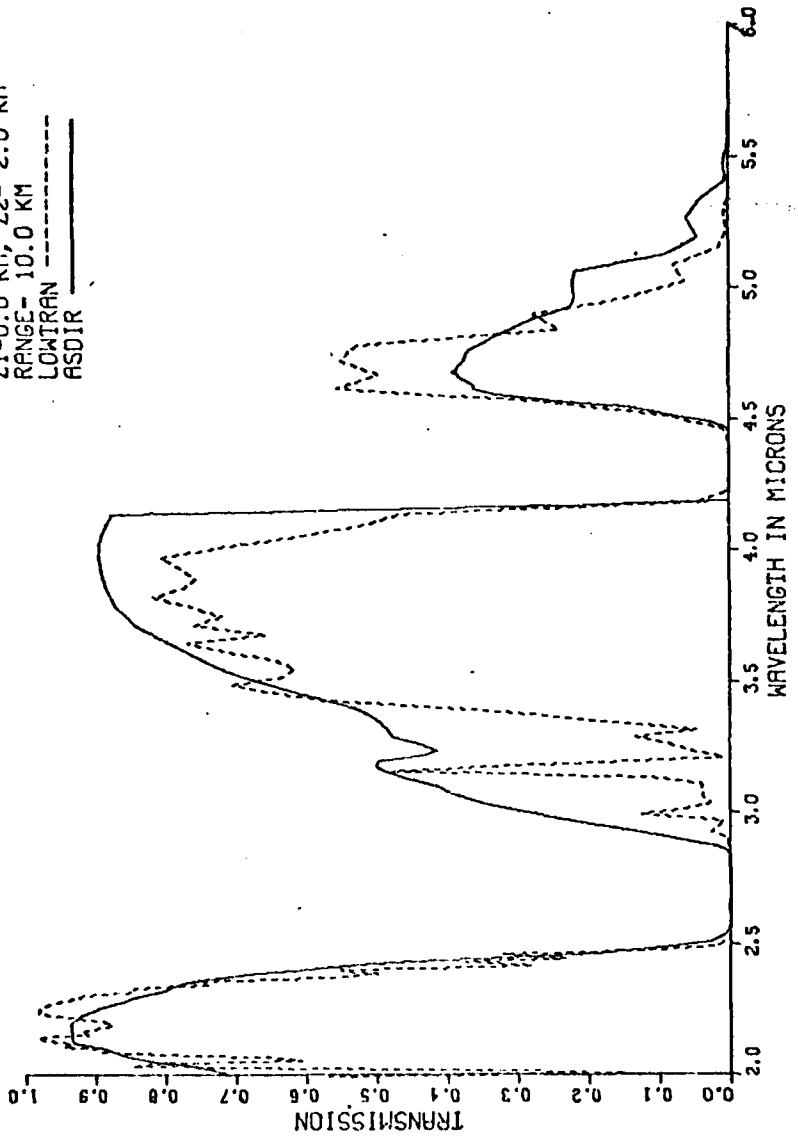


Figure 31. Low Altitude Comparison (Case 2) Between the Unmodified ASDIR and LOWTRAN Program Results

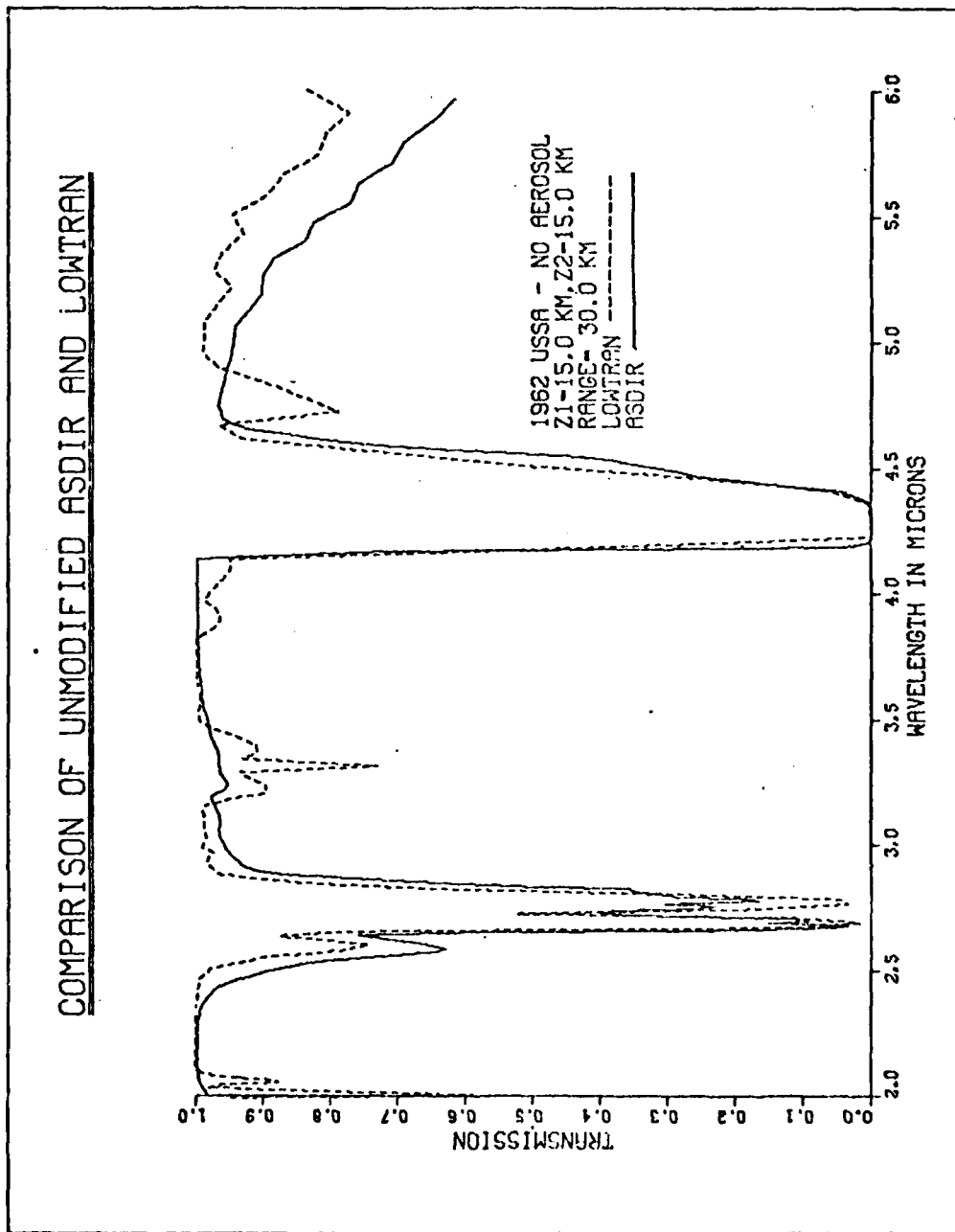


Figure 32. High Altitude Comparison (Case 3) Between the Unmodified ASDIR and LOWTRAN Program Results

the results validated by comparison with LOWTRAN. Figure 33 shows the comparisons of aerosol (only) transmission as predicted by the modified ASDIR and LOWTRAN programs for a short range, low altitude case using the average continental aerosol. Figure 34 compares total transmission plots from the two programs. Figures 35 and 36 are similar depictions assuming a maritime aerosol environment. Agreement between the modified ASDIR and LOWTRAN aerosol transmission is excellent while the total transmission shows the same differences as in Figs 30-32.

Note that for the 5 km visibility, representing a "hazy" condition, aerosol effects are seen to be a maximum at the lower wavelengths and decrease the overall transmission by 30 per cent or more in the 2.0-2.5 μm region. An analysis of these types of results indicate that on relatively clear days (of high absolute humidity) IR systems (eg. FLIR) of equivalent sensitivity will operate better in the 3-5 μm window while hazy conditions generally favor operation in the 8-12 μm region. It is specifically this kind of qualitative observation of system performance that the aerosol computations will help make when using ASDIR to compute target IR signatures.

Concluding Remarks

It is evident that the aerosol environment is one of the most important considerations in the overall performance of IR systems, especially at low altitudes. Aerosol

AEROSOL ONLY - ASDIR(MOD.) AND LOWTRAN

1962 USSA - AVG. CONT. AEROSOL
Z1-0.0 KM, Z2- 1.0 KM
RANGE- 4.0 KM
LOWTRAN -----
MODIFIED ASDIR _____
VIS - 5.0 KM

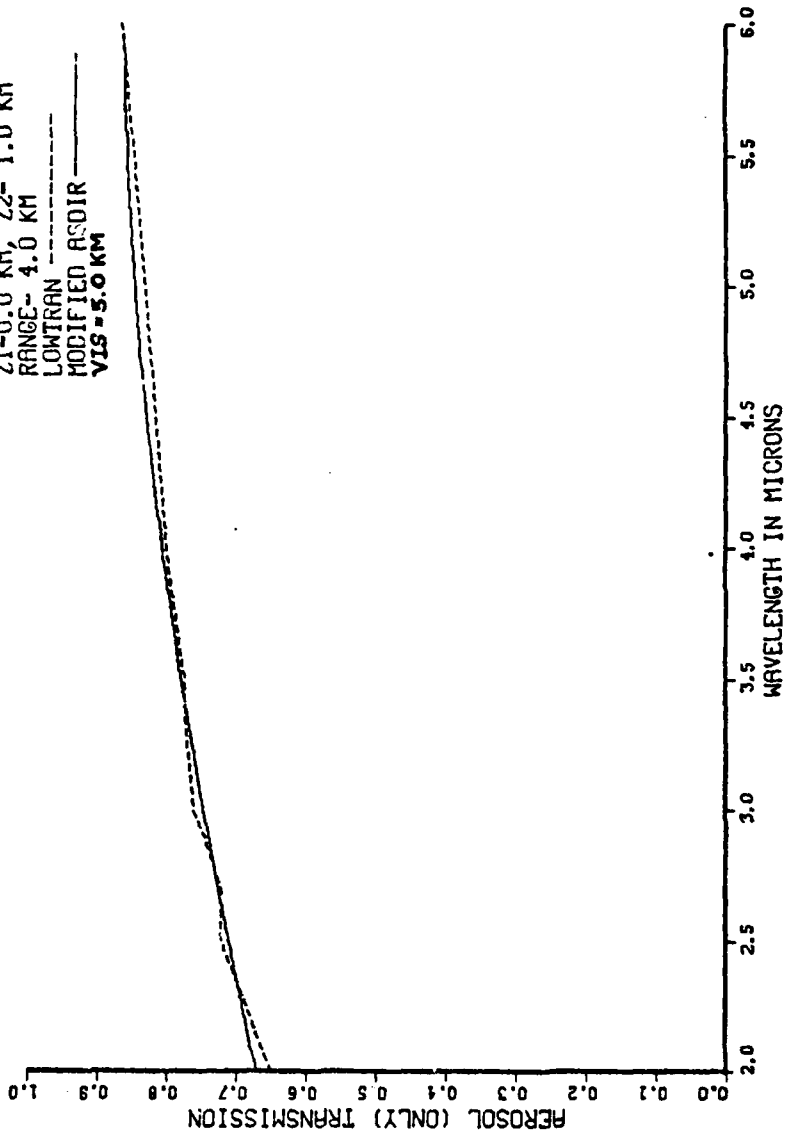


Figure 33. Modified ASDIR and LOWTRAN Comparison -
Aerosol Transmission (2-6 μ m)

MODIFIED ASDIR AND LOWTRAN COMPARISON

1962 USSA - AVG. CONT. ATMOSP.
VIS- 5.0 KM, Z1- 0.0 KM, Z2- 1.
RANGE- 4.0 KM
LOWTRAN - - - - -
MODIFIED ASDIR - - - - -

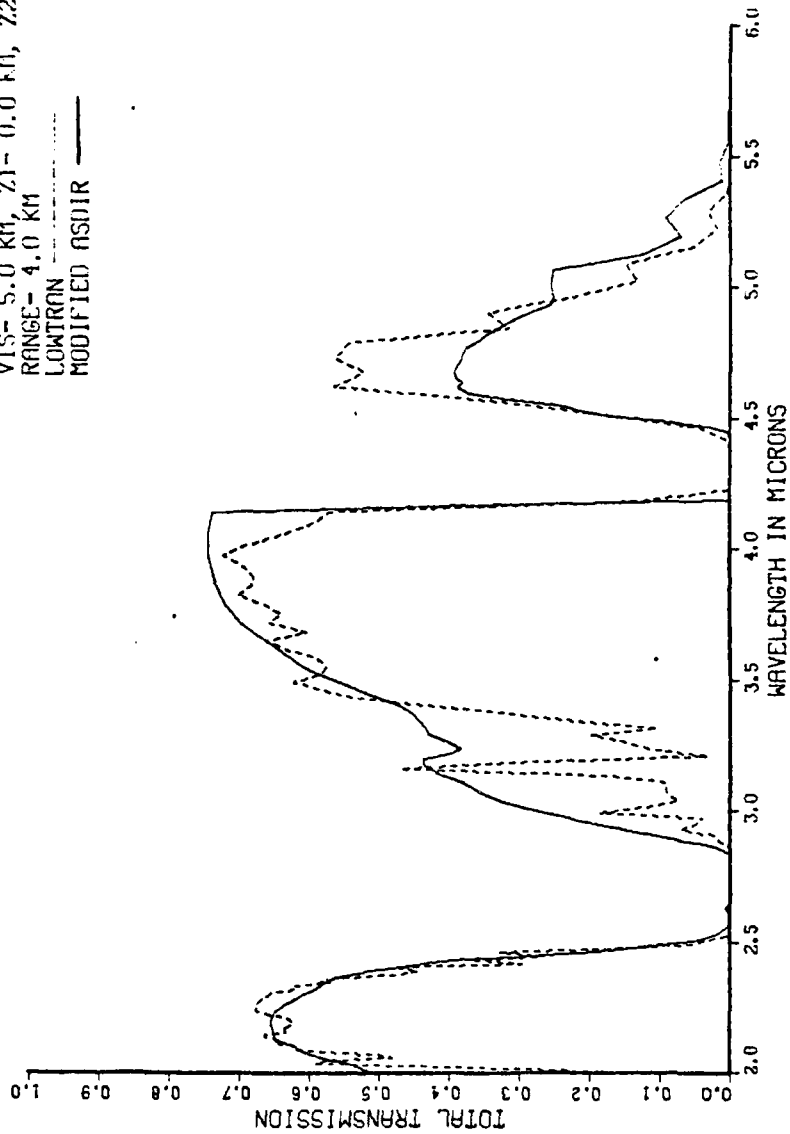


Figure 34. Modified ASDIR and LOWTRAN Comparison -
Total Transmission (2-6 μ m)

AEROSOL ONLY - ASDIR(MOD.) AND LOWTRAN

1962 USSA - MARITIME AEROSOL
Z1-0.0 KM, Z2- 1.0 KM
RANGE- 4.0 KM
LOWTRAN -----
MODIFIED ASDIR _____
VIS-5.0 KM

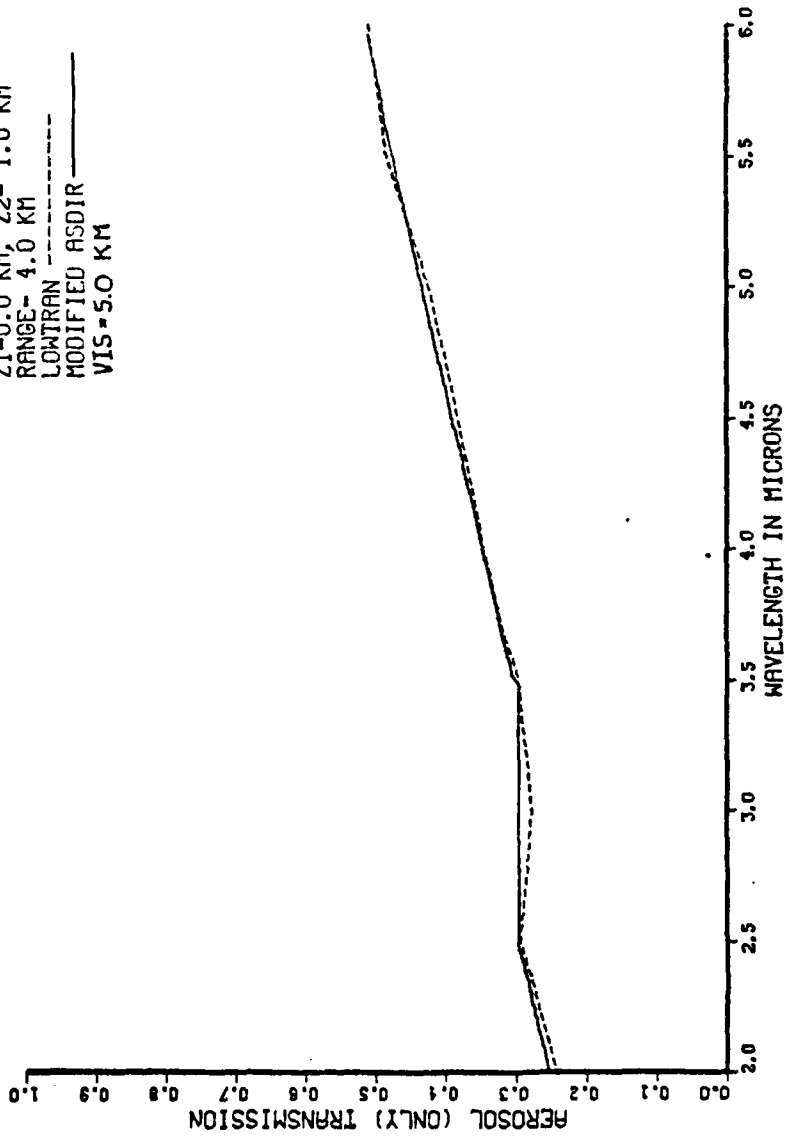


Figure 35. Modified ASDIR and LOWTRAN Comparison -
Aerosol Transmission (2-6 μ m)

MODIFIED ASDIR AND LOWTRAN COMPARISON

1962 USSA-MARITIME (AEROSOL)
VIS- 5.0 KM, ZI- 0.0 KM, Z2- 1.
RANGE- 4.0 KM
LOWTRAN -----
MODIFIED ASDIR -

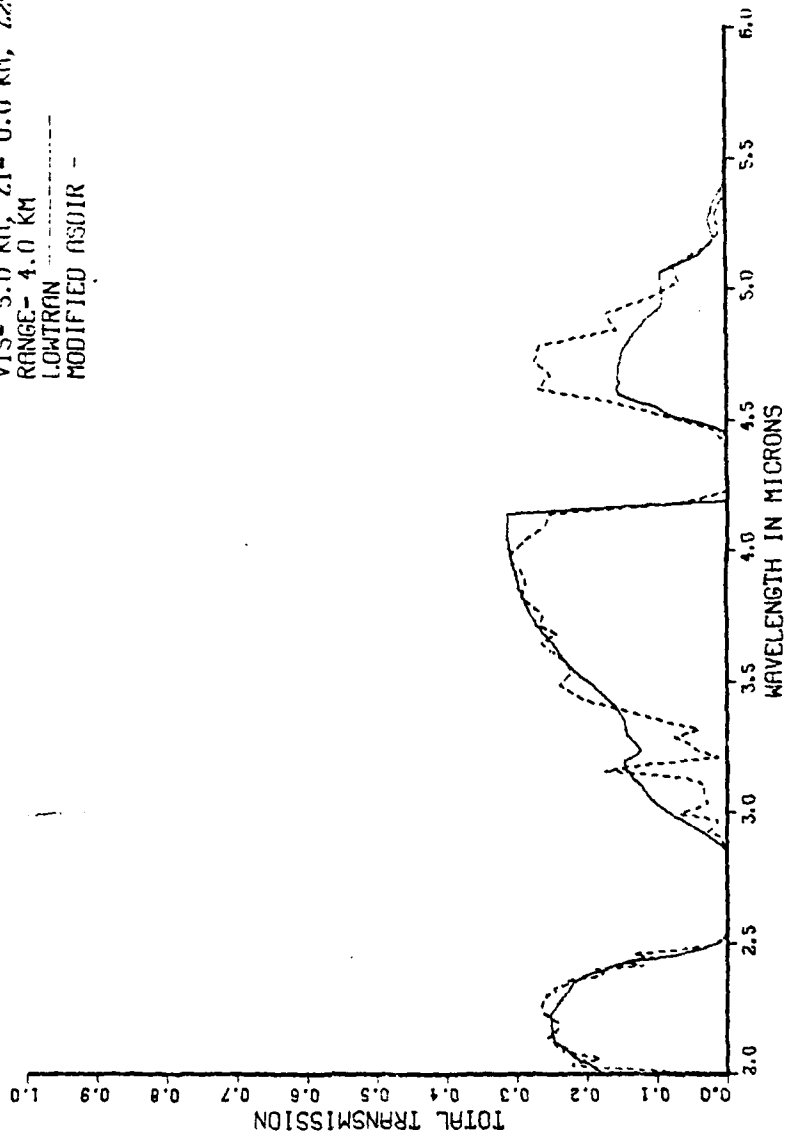


Figure 36. Modified ASDIR and LOWTRAN Comparison -
Total Transmission (2-6 μ m)

effects must be taken into account at every level of engineering design and evaluation of thermal imaging devices. The methods in this study to include aerosol computations into ASDIR represent a significant improvement in that program's capabilities. Additionally, the aerosol treatment here is quite flexible. As more accurate data on aerosols is obtained, this information can be incorporated into ASDIR through simple curve fits of the new extinction coefficients. The resulting analytical expressions can be inserted directly into the BETCAL portion (extinction coefficient calculations) called by the HAZE subroutine. Already, the latest edition of LOWTRAN includes such aerosol models as volcanic, radiation fog, advection fog, and high altitude (meteoric) aerosols. At least some of these will be installed into ASDIR by this writer in the following months.

Bibliography

1. Altshuler, T. L. "Infrared Transmission and Background Radiation by Clear Atmospheres," Doc. No. 61SD199. Valley Forge, PA: Missile and Space Vehicle Dept., General Electric Co., 1961.
2. Byers, H. R. Elements of Cloud Physics. Chicago: University of Chicago Press, 1965.
3. Cadle, R. D. Particles in the Atmosphere and Space. New York: Van Nostrand Reinhold, 1966.
4. Elterman, L. "Parameters for Attenuation in the Atmospheric Windows for Fifteen Wavelengths," Applied Optics, 3: 745-749 (1964).
5. ----- "UV, Visible, and IR Attenuation for Altitudes to 50 KM, 1968," Report AFCRL-68-0153. Bedford, MA: AFCRL, 1968.
6. Goody, R. M. Atmospheric Radiation: I, Theoretical Basis. London: Oxford University Press, 1964.
7. Hanél, G. "Properties of Atmospheric Particles as Functions of Relative Humidity, at Thermodynamic Equilibrium with the Surrounding Air," Advances in Geophysics, Vol. 19, New York: Academic Press, 1976.
8. Joint Tactical Coordinating Group/Air Survivability Handbook. JTCG, Washington, D.C.: Government Printing Office, 1977.
9. Junge, C. E. Air Chemistry and Radioactivity. New York: Academic Press, 1963.
10. McCartney, E. J. Optics of the Atmosphere: Scattering by Molecules and Particles, New York: Wiley and Sons, 1976.
11. McClatchey, R. A. et al. "Optical Properties of the Atmosphere," (revised) Report AFCRL-72-0497. Bedford, MA: AFCRL, 1972.
12. Middleton, W. E. K. Vision Through the Atmosphere. Toronto: University of Toronto Press, 1952.
13. Penndorf, R. "The Vertical Distribution of Mie Particles in the Troposphere," Report AFCRC-54-5. Bedford, MA: AFCRC, 1954.

14. Rensch, D. B. "Survey Report on Atmospheric Scattering," Report OSURF 2476-1. Columbus, OH: The Ohio State University Electro-Science Laboratory, 1968.
15. Roberts, R. E. "Atmospheric Transmission Modeling: Proposed Aerosol Methodology with Application to the Grafenwohr Atmospheric Optics Data Base," Paper P-1225, Arlington, VA: Institute for Defense Analysis, 1976.
16. Selby, J. E. A., and McClatchey, R. A. "Atmospheric Transmittance from 0.25 to 28.5 μm : Computer Code LOWTRAN 2," Report AFCRL-72-0745. Bedford, MA: AFCRL, 1972.
17. ----- "Atmospheric Transmittance from 0.25 to 28.5 μm : Computer Code LOWTRAN 3," Report AFCRL-75-0255. Bedford, MA: AFCRL, 1975.
18. Selby, J. E. A., et al. "Atmospheric Transmittance from 0.25 to 28.5 μm : Computer Code LOWTRAN 3," Report AFCRL-76-0258. Bedford, MA: AFCRL, 1978.
19. ----- "Atmospheric Transmittance from 0.25 to 28.5 μm : Computer Code LOWTRAN 4," Report AFCRL-78-0053. Bedford, MA: AFCRL, 1978.
20. Stone, C. and Tate, S. E. "ASDIR-II: Volume I, User's Manual," Report ASD/XR-75-1. Wright-Patterson AFB, OH: Aeronautical Systems Division, 1975a.
21. ----- "ASDIR-II: Volume II, Program Description," Report ASD/XR-75-1. Wright-Patterson, AFB, OH: Aeronautical Systems Division, 1975b.
22. ----- "ASDIR-II: Volume III, Reference Documentation," Report ASD/XR-75-1. Wright-Patterson AFB, OH: Aeronautical Systems Division, 1975c.
23. Stratton, J. A. Electromagnetic Theory. New York: McGraw Hill, 1941.
24. Van de Hulst, H. C. Light Scattering by Small Particles. New York: Wiley, and Sons, 1957.
25. Volz, F. E. "Infrared Refractive Index of Atmospheric Aerosol Substances," Applied Optics, 11: 755-759 (1972).
26. Walsh, J.L. Unpub. manuscript supplied by Mr. R.Gruenzel, Air Force Avionics Laboratory/RWI, Wright-Patterson AFB, OH, undated.

Appendix A

A Short Summary of Mie Theory and Calculations

The calculation of scattering and absorption of radiation by aerosol particles is very complex. Several fundamental assumptions are necessary if the problem is to be treated at all. This appendix briefly summarizes the highlights of Mie theory, undoubtedly the most widely used and experimentally verified tool for computing extinction due to small particles in the atmosphere.

The original work by Mie reported in 1908 resulted from basic research on scattering by colloidal metal particles. His theory found early applications in physical chemistry but applications to atmospheric optics were much slower to develop. In its complete form, Mie theory describes the scattering characteristics of a broad range of particle sizes and refractive indices. Additionally, the theory reduces to Rayleigh theory when the particles are small compared to the wavelength of the incident radiation. Thus, Rayleigh theory is simply a subset of the more general Mie theory and adequately describes the scattering by the very small gas molecules in the air - the scattering which accounts for the sky's blue color. Starting with the very small particles (molecular size), as the particle size relative to the wavelength increases, there is a gradual transition from Rayleigh to Mie scattering. Thus, the most important factor in Mie calculations is the

dimensionless size parameter α , defined by

$$\alpha = \frac{2\pi r}{\lambda} \quad (35)$$

where λ is the wavelength in the medium surrounding the particle and r is the particle radius. An important fact here is that the most significant factor, relative size, means that increasing the wavelength always results in making the particle appear smaller. Thus, a haze particle with a radius of 1 μm can be considered a relatively large particle when irradiated by visible light (approximately 0.55 μm) but becomes a relatively small one for, say, energy at 10.6 μm .

Next, one should note that Mie's theory solved the problem of a monochromatic plane wave incident on a homogeneous, isotropic sphere of radius r surrounded by a transparent homogeneous and isotropic medium. Thus, in using the theory we implicitly assume that the atmospheric particles are spherical and isotropic. That assumption, employed in this thesis by the use of LOWTRAN extinction coefficients calculated by Mie theory, is quite valid for wet haze particles such as fog and cloud droplets but certainly less valid for dust-like particles with their random shapes. However, scattering by non-spherical particles is extremely complex and this writer has encountered no practical applications of that case in the literature.

An atmospheric particle represents an optical

AD-A083 908

AIR FORCE INST OF TECH WRIGHT-PATTERSON AFB OH SCHOO
ADDITION OF AN AEROSOL TRANSMISSION MODEL TO THE AERONAUTICAL
MAR 79 A C MCLELLAN
AFIT/6AE/AA/79M-3

NL

UNCLASSIFIED

2 of 2

NO. 206390E



END
DATE
FILMED
6-80
DTIC

discontinuity to a light wave because the particle's refractive index is greater than that of the surrounding air. If the particle only scatters energy, with no absorption of the incident flux, then the index of refraction is a purely real number from about 1.33-1.60 (McCartney, 1976: 224). When absorption is significant, the index of refraction $m(\lambda)$ is represented as a complex number which can be written as

$$m(\lambda) = n_1(\lambda) - in_2(\lambda) \quad (36)$$

where n_1 and n_2 are the real and complex parts, respectively.

The index of refraction of particles is a very important parameter in atmospheric optics since it determines, in effect, the scattering and absorption cross sections for the aerosols. In the following section, the use of the size parameter and the index of refraction m to calculate the attenuation coefficients by Mie theory will be outlined. Much of this treatment can be traced back to Stratton's (1941) or Van de Hulst's (1957) work, and the interested reader is referred to those sources for more detailed development of the calculations for several other categories of radiation (eg. polarized energy). McCartney (1976) also gives an excellent summary of the theory and much of his treatment is condensed here.

The objective of these calculations is to compute an extinction coefficient for use in the Beer's law formulation

$$\tau_a = \exp(-\beta L) \quad (37)$$

where

τ_a = transmittance due to aerosols

L = equivalent path length of radiation

To accomplish this aim, it is first noted that the angular characteristics of Mie scattering for all particle sizes and wavelengths are expressed by two intensity distribution functions. The light scattered at an observation angle θ by a particle may be treated as consisting of two components having intensities $I_1(\theta)$ and $I_{11}(\theta)$. These components are proportional to two intensity distribution functions i_1 and i_2 , respectively. These functions represent the heart of Mie theory and depend on the size parameter α , the complex index of refraction m , and on the scattering angle θ . For a spherical, isotropic particle the intensity functions may be expressed as

$$i_1(\alpha, m, \theta) = \left| \sum_{n=1}^{\infty} \frac{2n+1}{n(n+1)} (a_n \pi_n + b_n T_n) \right|^2 \quad (38-a)$$

$$i_2(\alpha, m, \theta) = \left| \sum_{n=1}^{\infty} \frac{2n+1}{n(n+1)} (a_n T_n + b_n \pi_n) \right|^2 \quad (38-b)$$

where the n 's are positive integers; a_n and b_n are found from Ricatti-Bessel functions. The factors a_n and b_n have arguments formed from the particle characteristics α and m ,

but they are independent of the angle θ . The functions π_n and T_n in Eqs 38 depend only on the angle θ and involve the first two derivatives of Legendre polynomials having order n and argument $\cos \theta$. Extensive tabulations of these functions are formulated, especially since the advent of high speed computers, and are published in many sources.

When a particle is illuminated by unpolarized light, the scattered radiation consists of two incoherent components according to

$$I(\theta) = E_0 \frac{\lambda^2}{4\pi^2} \left(\frac{i_1 + i_2}{2} \right) \quad (39)$$

where i_1, i_2 are defined in Eqs 38 and E_0 is the irradiance of the incident light. Additionally, the angular cross section $\sigma_p(\theta)$ (also referred to as a particle scattering efficiency factor) may be defined as

$$\sigma_p(\theta) = \frac{I(\theta)}{E_0} = \frac{\lambda^2}{4\pi^2} \left(\frac{i_1 + i_2}{2} \right) \quad (40)$$

This factor $\sigma_p(\theta)$ is defined as that area such that the power flowing across it is equal to the scattered power per steradian at an observation angle θ . Equation 40 again applies only to unpolarized incident radiation; different relations written in terms of the polarized intensity components hold for polarized light.

Next, the total scattering cross section σ_p is defined

as that cross section of an incident wave acted upon by the particle having an area such that the power flowing across it is equal to the total power scattered in all directions. Thus, for a single particle

$$\sigma_p = \int_0^{4\pi} \sigma_p(\theta) d\omega \quad (41)$$

where $d\omega$ is a differential increment of steradian. Analogous cross sections can be defined for polarized incident light while Eq 41 holds for unpolarized radiation. Then, since

$$d\omega = 2\pi \sin \theta d\theta \quad (42)$$

we may perform the integration and define an efficiency factor Q_{sc} , which is the ratio of the scattering cross section to the geometric cross section, as

$$Q_{sc} = \frac{\sigma_p}{\pi r^2} = \frac{2}{r^2} \int_0^\pi \sigma_p(\theta) \sin\theta d\theta \quad (43)$$

The factor Q_{sc} defines the "efficiency" with which the particle totally scatters the incident light. From Eq 40 we see that

$$Q_{sc} = \frac{2}{r^2} \int_0^\pi \frac{\lambda^2}{4\pi^2} \left(\frac{i_1 + i_2}{2} \right) \sin\theta d\theta \quad (44-a)$$

$$Q_{sc} = \frac{1}{\alpha^2} \int_0^\pi (i_1 + i_2) \sin\theta \, d\theta \quad (44-b)$$

where α has previously been written as the dimensionless size ratio.

The integration in Eqs 44 is largely illustrative since for computational purposes i_1 and i_2 can be defined in terms of the complex functions a_n and b_n as shown in Eqs 38. In those terms σ_p can be written as

$$\sigma = \frac{\lambda^2}{2\pi} \sum_{n=1}^{\infty} (2n+1) (|a_n|^2 + |b_n|^2) \quad (45)$$

and the efficiency factor becomes

$$Q_{sc} = \frac{2}{\alpha^2} \sum_{n=1}^{\infty} (2n+1) (|a_n|^2 + |b_n|^2) \quad (46)$$

Both of these forms are well suited to calculation on digital computers.

In a method completely analogous to the previous development an extinction efficiency factor may be computed when the index of refraction has an imaginary part, i.e. when the particle absorbs energy. The result is

$$Q_{ext} = \frac{2}{\alpha^2} \sum_{n=1}^{\infty} (2n+1) \operatorname{Re}(a_n + b_n) \quad (47)$$

where Re denotes the real part of the sum of a_n and b_n .

Equations 46 and 47 compute the efficiency factors for a single particle. The extinction due to N identical particles of radius r in a volume is then

$$\beta_{\text{ext}} = N\pi r^2 Q_{\text{ext}} \quad (48)$$

where the area is πr^2 . Generally, as was discussed in Chapter II, there are many different sized particles in a volume, and thus the extinction coefficient for a collection of polydispersed spheres is

$$\beta_{\text{ext}} = \int_{r_1}^{r_2} \pi Q_{\text{ext}}(r) n(r) r^2 dr \quad (49)$$

where

$n(r)$ = the size distribution of the spheres

$Q_{\text{ext}}(r)$ = extinction efficiency at radius r

As shown in Chapter II the function $n(r)$ for aerosols is usually a smoothly varying one which may be described by a power-law distribution. Using the methods outlined here it can be understood how an aerosol size distribution can be assumed and, for a given index of refraction, extinction coefficients can be computed. This represents the methodology employed by the authors of the LOWTRAN code and adapted for use in this independent study.

Appendix B

Derivation of Expressions for Equivalent Path Lengths

To duplicate LOWTRAN's results several values of $AV(z, VIS)$ were obtained in successive runs of the LOWTRAN program. $AV(z, VIS)$ is described in Ref 11 as the equivalent sea level path length for aerosol extinction for vertical atmospheric paths. Use of the values of $AV(z, VIS)$ at each endpoint of a slant path is shown in Eq 34 where they are used to calculate the overall equivalent path length for the slant transmission path. AV values calculated by LOWTRAN are functions of both visibility and altitude for heights below 5 km through the dependence of the particle density upon visibility. Above 5 km the assumed particle densities are independent of visibility.

Figure 37 plots the results of LOWTRAN calculations for three visibilities from 0-7 km. As it appears in the figure there is a linear portion of each curve for constant VIS from $z=0$ to $z=3$. In the region $3 < z \leq 7$ the constant VIS curves are approximated by a parabola. All curve fits in this appendix were found using a HP-97 computer curve fit package capable of applying exponential, power, or logarithmic fits to sets of data. First the $z=0$ intercept was derived from a curve fit of $AV(0, VIS)$. The resulting expression was found as a power law fit:

$$AV(0, VIS) = 25.952 VIS^{-1.037} \quad (50)$$

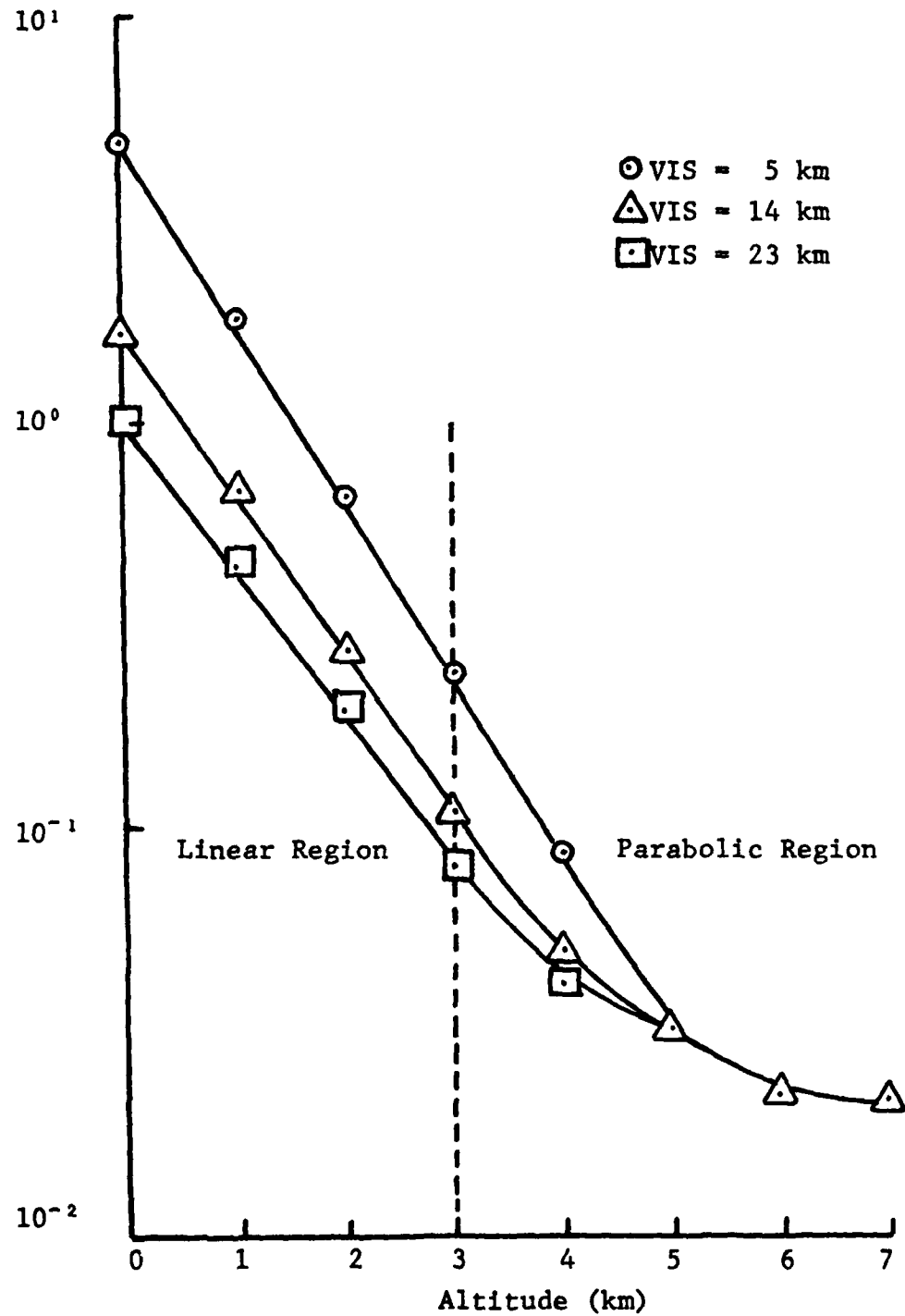


Figure 37. LOWTRAN Values of Equivalent Sea Level Path Lengths for Vertical Paths (AV(z))

Next, an expression for the slope (SLP) of the constant VIS curves in the linear region ($z \leq 3$) was found. Here a logarithmic curve fit given by Eq 51 produced a good fit to the data.

$$\text{SLP} = -1.187 + 0.106 \ln (\text{VIS}) \quad (51)$$

Combining the two previous expressions gives a function for computing $\text{AV}(z, \text{VIS})$ in the linear region given by Eq 52.

$$\begin{aligned} \text{AV}(z, \text{VIS}) &= \text{AV}(0, \text{VIS}) \exp(\text{SLP} \times z) \\ &= 25.952 \text{VIS}^{-1.037} \exp((-1.187 + 0.106 \ln \text{VIS})z) \end{aligned} \quad (52)$$

In the region $3 < z \leq 7$ a parabolic approximation was developed from the standard formula for a parabola where h, k are coordinates of the parabola's vertex:

$$(y-k) = c(x-h)^2 \quad (53)$$

In the present case the parabola's vertex is taken as $(7, \ln \text{AV}(7, \text{VIS}))$ or $(7, 0.021)$. The constant c is found for each curve (given by VIS) by matching the parabola to the straight lines at $\text{AV}(3, \text{VIS})$. The resulting expression for $\text{AV}(3, \text{VIS})$ computed using the linear region formula (Eq 52) is

$$\text{AV}(3, \text{VIS}) = (25.952 \text{VIS}^{-1.036}) \exp(-3.559 + 0.312 \ln \text{VIS}) \quad (54)$$

Substituting these expressions into the general equation for

the parabola a simplified expression for $AV(z, VIS)$ in the parabolic region is

$$AV(z, VIS) = 0.0208 \left(\frac{AV(3, VIS)}{0.0208} \right) \left(\frac{7.0 - z}{4} \right)^2 \quad (3 < z \leq 7) \quad (55)$$

For altitudes above 7 km the following functions were found to give satisfactory approximations for $AV(z)$:

$$\begin{aligned} 7.0 < z \leq 18.5 \text{ km} & \quad AV(z) = 10^{(-0.0148z + 1.549)} \\ 18.5 < z \leq 20.0 \text{ km} & \quad AV(z) = 10^{(-0.136z + 0.692)} \\ 20.0 < z & \quad AV(z) \text{ assumed zero} \end{aligned} \quad (56)$$

Appendix C

Program Listing of Subroutines HAZE, AVCAL, and BETCAL

```

SUBROUTINE HAZE(R,Z1,Z2,MODEL,VIS,NU,TAUH)
COMMON IFLAG
REAL LAM
C*****MODEL=1 FOR LOWTRAN AVG. CONTINENTAL AEROSOL MODEL *
C *MODEL=2 FOR LOWTRAN MARITIME AEROSOL MODEL *
C *NU=FREQUENCY (CM-1) *
C*****
ACON(A,B,C,D,Z)=.388*(A*10.**(-B*Z)-C*10.**(-D*Z))
BCON(A,B,C,D,Z)=(5.7*(A*10.**(-B*Z))-23.*(C*10.**(-D*Z)))/18.
IF(VIS.LT.3.0) MODEL=2
LAM=1.0E04/NU
IFLAG=IFLAG+1
IF(IFLAG.NE.1) GO TO 500
IF(VIS.GE.3.0) GO TO 5
PRINT*,"*****"
PRINT*,"LOW VISIBILITY INDICATES POSSIBLE FOG CONDITIONS **"
PRINT*,"LOWTRAN MARITIME AEROSOL MODEL BEING USED **"
PRINT*,"*****"
5 CONTINUE
PNO=2E23
C***DETERMINE IF THE PATH IS HORIZONTAL OR SLANT
IF(AIS(Z1-Z2).GT.0.5) GO TO 100
C***COMPUTE AHZ FOR THE HORIZONTAL PATH
IF(Z1.GE.0.0.AND.71.LE.3.0) GO TO 10
IF(Z1.GT.3.0.AND.71.LE.4.0) GO TO 20
IF(Z1.GT.5.0) GO TO 40
IF(Z1.GT.4.0.AND.71.LE.5.0) GO TO 30
10 AC=ACON(13780,0.437,2828,0.36,Z1)
BC=BCON(13780,0.437,2828,0.36,Z1)
GO TO 50
20 AC=ACON(13780,0.437,1529,0.277,Z1)
BC=BCON(13780,0.437,1529,0.277,Z1)
GO TO 50
30 AC=ACON(13780,0.437,422,0.137,Z1)
BC=BCON(13780,0.437,422,0.137,Z1)
GO TO 50
40 IF(71.LE.6.) GO TO 41
IF(Z1.GT.6.0.AND.71.LE.18.0) GO TO 42
IF(Z1.GT.18.0.AND.71.LE.30.) GO TO 43
AHZ=C.0
GO TO 500
41 FN=422.*10.**(-.137*Z1)
GO TO 60
42 PN=76.8*10.**(-0.0139*Z1)
GO TO 60
43 PN=3651.*10.**(-0.0107*Z1)
GO TO 60
50 PN=AC/VIS-BC
60 AHZ=PN*R/PNO
AHZ=AHZ*.905
PRINT*,"THE PATH IS APPROXIMATELY HORIZONTAL"
PRINT*,"THE EPL IS ",AHZ
GO TO 500
100 CONTINUE
C***COMPUTE THE EQUIVALENT SEA LEVEL PATH LENGTH FOR SLANT PATH
PRINT*,"THE PATH IS A SLANT PATH"
CALL AVCAL(Z1,VIS,AV)
AV1=AV
PRINT*,"Z1= ",Z1," AV1(KM-1)= ",AV1
CALL AVCAL(Z2,VIS,AV)

```

```

AV2=AV
PRINT*, "Z2= ", Z2, "      AV2(KM-1)= ", AV2
AHZ=ABS((AV1-AV2)*R/(Z1-Z2))
IF (Z1.GT.5.0.AND.Z2.GT.5.0) GO TO 200
CFAC=-0.0435*(VIS**2)+2.397*VIS-13.52
CFAC=CFAC/100.0
CFAC=1.0+CFAC
AHZ=AHZ*CFAC
GO TO 300
200  AHZ=(AV1+AV2)/2.0
300  PRINT*, "THE EQUIVALENT PATH LENGTH IS ", AHZ
500  CONTINUE
C*** COMPUTE TAU, THE TRANSMISSION AT WAVELENGTH LAM
***** COMPUTE THE EXTINGUISHING COEFFICIENT BY A CALL TO BETCAL
      CALL BETCAL(LAM, MODEL, PET)
C*** COMPUTE THE OPTICAL DEPTH
      OD=BET*AHZ
C*** COMPUTE TAU
      TAU=EXP(-OD)
      RETURN
      END

```

```

C***** *****
SUBROUTINE AVCAL(Z,VIS,AV)
C *****
C *THIS SUBROUTINE COMPUTES THE EQUIVALENT SEA LEVEL PATH LENGTH
C *(PER KM) FOR SLANT PATHS. REFER TO FIG. 15 IN OPTICAL PROPERTIES
C *OF THE ATMOSPHERE BY MCCLATCHY, ET AL (1972). AV(Z) FOR Z LESS
C *THAN 7 KM HAS BEEN DERIVED BY SYSTEMATIC CURVE FITS OF LOWTRAN
C *COMPUTED VALUES AS A FUNCTION OF BOTH VIS AND ALTITUDE (Z)
C *****
      IF (Z.LE.3.0) GO TO 10
      IF (Z.GT.3.0.AND.Z.LE.7.0) GO TO 20
      IF (Z.GT.7.0.AND.Z.LE.18.35) GO TO 30
      IF (Z.GT.18.35.AND.Z.LE.20.0) GO TO 40
      IF (Z.GT.20.0) AV=0.0
      RETURN
10  CONTINUE
C** COMPUTE THE VALUE OF AV(C,VIS)--THE Y INTERCEPT OF AV
      AVC=(25.951766*VIS**(-1.036584))
C** COMPUTE THE SLOPE (SLP) OF THE AV CURVE AS FUNCTION OF VIS
      SLP=-1.1065563 + 0.1056718*ALOG(VIS)
C** COMPUTE AV(Z,VIS) IN THE LINEAR REGION
      AV=AVC*EXP(SLP*Z)
      RETURN
20  CONTINUE
C** COMPUTE VALUE OF AV(3,VIS)
      AV3=(25.951766*VIS**(-1.036584))*EXP(-3.559675+.312134*ALOG(VIS))
C** COMPUTE AV(Z,VIS) IN THE PARABOLIC REGION
      POW=((7.0-Z)/5.0)**2
      AV=0.0206*((AV3/.0210)**(POW))
      RETURN
30  AV=10.0**(-0.01477*Z+1.549)
      RETURN
40  AV=10.0**(-0.136*Z+0.692)
      RETURN
      END

```

```

SUBROUTINE BETCAL (HLAM, M, BET)
C *****
C * BETCAL COMPUTES THE EXTINCTION COEFFICIENT AS A FUNCTION OF *
C * WAVELENGTH LAM FOR TWO OF THE LOWTRAN ATMOSPHERIC AEROSOL *
C * MODELS. M=1 USES THE AVERAGE CONTINENTAL MODEL. M=2 USES *
C * THE MARITIME MODEL. THE MARITIME MODEL SHOULD NORMALLY BE *
C * USED FOR LOW VISIBILITY CONDITIONS (VIS LESS THAN 5 KM) SINCE *
C * FOG CONDITIONS MAY BE PRESENT. *
C *****
COMMON IFLAG
REAL LAM
LAM=HLAM
IF (M.EQ.2) GO TO 10
IF (IFLAG.EQ.1) PRINT*, " USING AVG. CONTINENTAL MODEL"
IF (LAM.GE.0.86.AND.LAM.LE.2.0) BET=-0.06391*LAM+0.162995
IF (LAM.GT.2.0.AND.LAM.LT.7.2) BET=0.0012*LAM**(2.)-0.01474*LAM
C+0.017545
IF (LAM.GE.7.2.AND.LAM.LT.7.9) BET=-7.8E-03*LAM+6.946E-02
IF (LAM.GE.7.9.AND.LAM.LE.8.2) BET=8.33E-04*LAM+1.2567E-03
IF (LAM.GT.8.2.AND.LAM.LE.9.0) BET=-8.79E-03*LAM**(2.)
C+0.17665*LAM-0.91175
IF (LAM.GT.9.0.AND.LAM.LE.9.2) BET=0.02365
IF (LAM.GT.9.2.AND.LAM.LE.14.0) BET=0.010557-1.147E-04*LAM
C+138.538*EXP(-LAM)
IF (LAM.GT.14.0) BET=0.010
RETURN
10 CONTINUE
C*****MARITIME AEROSOL MODEL EXTINCTION COEFFICIENTS
IF (LAM.GE.0.86.AND.LAM.LE.2.5) BET=-0.02134*LAM+0.167455
IF (LAM.GT.2.5.AND.LAM.LE.3.5) BET=0.0999
IF (LAM.GT.3.5.AND.LAM.LE.8.2) BET=0.00221*LAM**(2.)
C-0.03816*LAM+0.214351
IF (LAM.GT.8.2.AND.LAM.LT.9.0) BET=-0.010133*LAM**(2.)
C+0.17739*LAM-0.733659
IF (LAM.GE.9.0.AND.LAM.LT.11.0) BET=0.002523*LAM**(2.)-0.0612*LAM+
C.3804
IF (LAM.GE.11.0.AND.LAM.LE.14.0) BET=0.0640E*LAM-0.01996
IF (LAM.GT.14.0) BET=0.039
IF (IFLAG.EQ.1) PRINT*, "MODEL=2 (MARITIME AEROSOL MODEL)"
RETURN
END

```

Vita

Captain Allen Clifton McLellan was born on 23 February 1947 in Memphis, TN. He graduated from the Harding Academy of Memphis in June 1965, and entered Mississippi State University in September of the same year. As a sophomore cadet in AFROTC at "State" he was appointed to the United States Air Force Academy from which he graduated in June 1971. Next came attendance at USAF Undergraduate Navigator Training which he completed in April 1972 and was named a Distinguished Graduate. Then followed a 13 month assignment as a navigator and instructor navigator in the C-141A stationed at Charleston AFB, South Carolina. It was there that he met and later married the former Glenda Faye Perry. In 1973 Captain McLellan entered training as an RF-4C Weapon Systems Officer (WSO) and served a 40 month tour at Kadena Air Base, Japan, as a WSO, instructor, and flight examiner. While stationed at Kadena he returned to the CONUS in March 1976 for attendance at Squadron Officers' School from which he was named a Distinguished Graduate. Captain McLellan entered the Air Force Institute of Technology in August 1977.

Permanent Address: Rt 2, Box 191
Ashland City, TN 37015

UNCLASSIFIED

SECURITY CLASSIFICATION OF THIS PAGE (When Data Entered)

REPORT DOCUMENTATION PAGE		READ INSTRUCTIONS BEFORE COMPLETING FORM
1. REPORT NUMBER AFIT/GAE/AA/79M-3	2. GOVT ACCESSION NO. AD-A083 908	3. RECIPIENT'S CATALOG NUMBER
4. TITLE (and Subtitle) ADDITION OF AN AEROSOL TRANSMISSION MODEL TO THE AERONAUTICAL SYSTEMS DIVISION INFRA-RED EMISSION PREDICTION PROGRAM (ASDIR)		5. TYPE OF REPORT & PERIOD COVERED MS Thesis
		6. PERFORMING ORG. REPORT NUMBER
7. AUTHOR(s) Allen C. McLellan Captain, USAF		8. CONTRACT OR GRANT NUMBER(s)
9. PERFORMING ORGANIZATION NAME AND ADDRESS Air Force Institute of Technology (AFIT-EN) Wright-Patterson AFB, Ohio 45433		10. PROGRAM ELEMENT, PROJECT, TASK AREA & WORK UNIT NUMBERS
11. CONTROLLING OFFICE NAME AND ADDRESS Aeronautical Systems Division/XRE Wright-Patterson AFB, Ohio 45433 Attn: Mr. Stan Tate		12. REPORT DATE March, 1979
		13. NUMBER OF PAGES 99
14. MONITORING AGENCY NAME & ADDRESS (if different from Controlling Office)		15. SECURITY CLASS. (of this report) Unclassified
		15a. DECLASSIFICATION DOWNGRADING SCHEDULE
16. DISTRIBUTION STATEMENT (of this Report) Approved for public release; distribution unlimited		
17. DISTRIBUTION STATEMENT (of the abstract entered in Block 20, if different from Report)		
18. SUPPLEMENTARY NOTES Approved for public release; IAW AFR 190-17 JOSEPH P. HIPPS, Major, USAF Director of Information		
19. KEY WORDS (Continue on reverse side if necessary and identify by block number) Infrared Signatures Aerosol Attenuation Atmospheric Transmission		
20. ABSTRACT (Continue on reverse side if necessary and identify by block number) The Aeronautical Systems Division Infra-Red Emission Program (ASDIR) is a large computer program compiled in 1974-75 using a "state of the art" routines to predict hot surface and plume emissions from a geometrically modeled target. The atmospheric transmission segment of the program included only the major gaseous absorbers (H ₂ O, CO ₂ , and N ₂ O) with no aerosol attenuation. To improve the flexibility of the program in making more accurate predictions at low altitudes, an aerosol transmission computational		

UNCLASSIFIED

SECURITY CLASSIFICATION OF THIS PAGE(When Data Entered)

↙ scheme was written for the ASDIR code.

Using the basic methodology in the ~~Air Force Geophysics~~
~~Laboratory~~ (AFGL) transmission model LOWTRAN 4, a subroutine, was written for direct inclusion into ASDIR. Curve fits of the following LOWTRAN parameters were performed which simplified the aerosol procedures and minimized the additional computer storage and time requirements in ASDIR: (1) assumed aerosol particle densities, (2) equivalent sea level path lengths for vertical paths - $AV(z)$, and (3) total sea level extinction coefficients for an "average continental" and "maritime" aerosol models. Results of the new subroutine (called HAZE) compared very well with LOWTRAN's aerosol predictions. A logic change was included in HAZE to automatically select a maritime aerosol model under low visibility conditions. This programming change was prompted by results of a recent Grafenwohr, FRG transmission study. ↑

UNCLASSIFIED

SECURITY CLASSIFICATION OF THIS PAGE(When Data Entered)